UNCERTAINTY IN FISH LOCATION USING A SPLIT BEAM SONAR

By

Mark L. Ayers

RECOMMENDED:

Joseph L. Hedrick

John J. Kelley

C. S. Sonnerville

Advisory Committee Chair

John Aspres

Department Head

APPROVED:

D. Woodall

Dean, College of Science, Engineering and Mathematics

Dean of the Graduate School

4-10-01

Date

Uncertainty in Fish Location using a Split Beam Sonar

A

THESIS

Presented to the Faculty
of the University of Alaska Fairbanks

in Partial Fulfillment of the Requirements
for the Degree of

MASTER OF SCIENCE

By
Mark L. Ayers, B.S. Mathematics

Fairbanks, Alaska

May 2001

Abstract

The enumeration of fish is of critical importance to the management of both commercial and sport fisheries in Alaska and worldwide. Current methods for riverine fish enumeration are inaccurate and unreliable. Improved fish counting accuracy in Alaskan rivers by acoustic methods is required.

A split beam sonar system in the presence of noise is modeled. The sonar system including the received sonar pulse, receiver system, transducer beam pattern, propagation losses, and noise are modeled. An analysis of the effects of noise, pulse duration and sampling frequency on the uncertainty in fish location is presented.

Signal to noise ratios less than 5 dB can cause significant errors in the calculation of received signal phase. A stationary fish with a signal to noise ratio of 15 dB has approximately $\pm$ 0.001 degrees of uncertainty in the angles of arrival. Reducing the SNR to 3 dB the uncertainty increases to $\pm$ 3.6 degrees in the angles of arrival.

Contents

List of Figures

List of Tables

Acknowledgments

This thesis is dedicated to my wife Terra for all of her love and support during the busy, hectic time while I wrote this thesis. Her love and care for me are what allowed me to succeed as a student and a husband.

Thanks to my parents and family for supporting me in my goals. My success is not simply my own doing, but the consolidation of support, love, prayers and education that has been provided by all of my family and friends.

A great deal of appreciation is due to my thesis advisor, Professor Vikas S. Sonwalkar. The help and guidance that Vikas provided me throughout my time at UAF was exceptional. In addition to providing the necessary academic education, Vikas also gave me the skills to succeed as a professional engineer. The dedication that Vikas exhibits towards the students that work for him is something that I will strive to mimic in my own professional career. I not only consider Vikas a great professor and advisor, but also a friend. Thank you Vikas.

I would also like to thank the other members of my thesis committee, Professor John Kelley and Professor Joe Hawkins. The encouragement and excitement that John Kelley showed me during my research is something I have seldom seen in my life. I am grateful Professor Hawkins for his initial interest in my application to the Electrical Engineering program at UAF. If it were not for his input and help, I may have never attended UAF.

Thanks to everyone else who helped me in any way to complete this milestone in my career as a student. Thanks especially to John Pham, a fellow graduate student whose work this thesis is based on. Thanks to Barbara Adams, for providing me with resources and results which I used directly in my thesis.

Lastly, I would like to thank God for all of the gifts and talents He has endowed

me with. I am aware of many instances while I pursued my education that I could feel his presence. Without my faith, I would have failed long ago.

This work was partially supported by a grant (ASTF, Grant 97-4-147) from the Alaska Science and Technology Foundation.

1 Introduction

The enumeration of fish is of critical importance to the management of both commercial and sport fisheries in Alaska and worldwide. Current methods for fish enumeration and sonar counting are inaccurate and unreliable. Tower counts are not practical for large scale surveys and are only usable in clear, shallow river conditions, a rarity in Alaska. Careful examination is required to improve the accuracy of fish counts in Alaskan rivers using acoustic methods.

1.1 Scientific Background

Several different methodologies [MacLennan et al., 1992] exist for using sonar to count fish. The oldest and most widely used is the single beam sonar. Early systems consisted of a transmitter/receiver, a pulse generator, and a chart recorder. In this configuration, a pulse is transmitted and the receiver waits for returned echoes. The echoes are recorded with the chart recorder, with darker marks corresponding to higher target strengths. The returned echoes are arranged on the chart as a function of target range. Early systems provided only a qualitative measure of fish or biomass density. As electronics technology progressed, the single beam systems became more sophisticated. Current single beam echosounders use color displays and variable frequencies to provide better visualization of the fish. Color displays make classifying different returned echo levels much easier for the novice user. Variable frequencies allow the user to choose a signal with a wavelength that is appropriate to the fish and medium.

Counting fish populations using a single beam sonar can be done using techniques called echo integration and echo counting

[MacLennan et al., 1992]. These two commonly used (indirect) methods for obtaining stock size estimates depend on the acoustic size of the individual fish [Ehrenberg 1981]. Echo integration is a simple technique where all of the energy in the returned echoes is summed. This integrated energy is then divided by an average energy expected for one fish, providing a more quantitative measure of the number of fish present. Several problems exist with echo integration. The sea bed must be removed from the echoes to be integrated, which can lead to errors if the fish being counted are near the sea bed. The average fish echo energy that is assumed can lead to large errors in the fish count because fish target strength can vary by as much as 30 dB depending on the orientation of the fish in the transducer beam. In the case of fish which are sparsely distributed in the water, as opposed to clumped in schools or layers, it may be possible to detect the echoes from individual fish. The count of these echoes might be used to determine the density of fish within the acoustic beam[MacLennan et al., 1992].

The indirect techniques of fish counting are susceptible to numerical and statistical errors and do not work well in many cases of interest [Traynor and Ehrenberg 1990].

In order to better quantify the target strength of individual fish, the direction of arrival of the returned echo is measured. Knowledge of the direction of arrival of the returned echo allows the system to compensate for the transducer beam factor and allows individual fish to be tracked. Furthermore, the angular location data provided with split-beam systems can also be used in conjunction with the tracking data for fixed location acoustic systems to provide estimates of fish swimming speed, location in the water column, and direction of travel [Ehrenberg and Torkelson 1996]. Two sonar systems are commercially available for performing these measurements. The dual-beam sonar echosounder uses a wide beam and a narrow beam transducer to obtain an target strength estimate. The narrow beam transducer is used to transmit

the pulse, and both the wide and narrow beam receivers listen for an echo. The echoes reflected from single fish are received simultaneously on the narrow-beam and wide-beam transducers [Traynor and Ehrenberg 1990]. The effects of the transducer beam factor are then removed providing a better estimate of the fish target strength. The split beam sonar system extends the dual-beam system to four receivers. In the split beam case, four receivers listen for returned echoes. In the split beam system, the use of four receivers allows left/right and up/down angle of arrival measurements. It has been shown that, in theory, the split beam system will have superior performance to the dual beam in the presence of noise [Traynor and Ehrenberg 1990]. There can often be a considerable amount of reverberation present in the received signals [Ehrenberg and Torkelson 1996]. Reverberation noise, in conjunction with background and receiver noise can corrupt the received signal and produce errors in the phase and time delay measurements. The split beam system is more difficult to implement than the dual beam technique. The hardest part (of the split beam system) is implementing the hardware and/or software for measuring the phase difference between the signals received on the two half beams [Ehrenberg 1983]. The quality of the backscattering cross section estimates obtained using the split beam system will be determined by the quality of the measurements of the up/down and left/right angles of arrival measurements [Ehrenberg 1981]. A better understanding of split beam sonar is thus required for reliable measurement of fish counts in Alaskan rivers.

1.2 Contributions of present work

This research concerns the modeling of a split beam sonar system in the presence of reverberation modeled as Gaussian random noise. Analysis and interpretation of the

modeled signals is presented. The objective of the first part of this thesis is to present a realistic model for the split beam sonar system. The received sonar pulse, receiver system including transducer beam pattern, propagation losses and noise are modeled. The transmitted sonar pulse is modeled as a rectangular pulse with finite rise and fall times modulated with a cosine waveform at a given frequency. The receiver system is modeled as a rectangular array of 4 identical receivers. Spreading loss, beam factor and fish orientation are also modeled. Noise is modeled as a Gaussian random process with zero mean and standard deviation based on the signal to noise ratio.

The second part of the thesis is an analysis of the effects of noise on the uncertainty in fish location. The effects of pulse duration and sampling frequency are discussed. Fish uncertainty is examined by simulating a stationary fish and obtaining samples of the fish location estimate in the presence of noise. Simulating the target location in this manner produces a range of possible fish locations that represent the range of uncertainty in the estimate. We give examples of fish tracks with known positions. The fish track is simulated with noise and the uncertain locations are presented. Fish tracks are also simulated and compared with data collected in 1995 from Chandalar River, Alaska. This data provides [x y z] fish coordinates as well as beam factor and target strength estimates.

We show that noise in the split beam system can be a significant source of error in the calculation of the returned phase when the signal to noise ratio is less than 5 dB. For a stationary fish with a signal to noise ratio of 15 dB, the uncertainty in the location estimate is approximately $\pm$ 0.001 degrees in the left/right and up/down arrival angles. Decreasing the signal to noise ratio to 3 dB causes the uncertainty in arrival angle to increase to $\pm$ 3.6 degrees. The errors in the case where the signal to noise ratio is 15 dB are due only to phase measurement errors, while the errors in the

3 dB case are due to both phase measurement and range estimate errors which lead to phase wrap. Both of the range and phase must be measured accurately to obtain an accurate fish location estimate.

The thesis is organized as follows, Chapter 2 presents a description of the split beam sonar system and the model developed, Chapter 3 is an analysis of the split beam system using the model developed, Chapter 4 is the Conclusions and Discussion of results including suggestions for further research, Chapter 5 is an Appendix containing the derivations used in the sonar model. The numerical simulations provided in this thesis were performed using Matlab software. A listing of the source code for Matlab M-files used to perform various simulations as well as how they are used to calculate various parameters are provided in a separate report [Ayers 2001].

2 Sonar System Model

2.1 Description of a Split Beam Sonar

2.1.1 Objective and Geometry of Sonar Model

The objective of the split beam system model is to determine fish location using simulated fish echo data. The split beam echosounder has a transducer which is divided into four quadrants as shown in figure 1. The target direction is determined by comparing the phase of the signals received by each quadrant. The transmission pulse is applied to the whole transducer, but the signals received by each quadrant are processed separately. Suppose the four quadrants are labeled '1' to '4' as in figure 1. The angle θ_1 to the target in X_R-Z_R plane is determined by the phase differences (1 - 2) and (3 - 4), which should be the same. Thus the summed signal (1 + 3) is compared with (2 + 4) in the simulations. The angle θ_2 is in Y_R-Z_R plane and is similarly determined by the phase difference between (1 + 2) and (3 + 4). The two angles define the target location uniquely. The target strength is estimated from the transducer sensitivity in the relevant direction, namely the beam pattern which is determined by calibration. There are two sources of directional uncertainty in the split beam sonar system. Uncertainties in the measured phase due to noise can cause inaccurate fish location measurements. Ambiguities in the received phase due to phase wrap can also lead to error in the fish location measurements. Suppose the difference in the path lengths from quadrants '1' and '2' to a particular target location is D. If the path length difference for another target location is $D + \lambda$, the relative phase of the two signals would be the same. This problem can be avoided to a large extent by good transducer design and the application of thresholds which the detected signals must exceed [MacLennan et al., 1992]. The measured phase is used

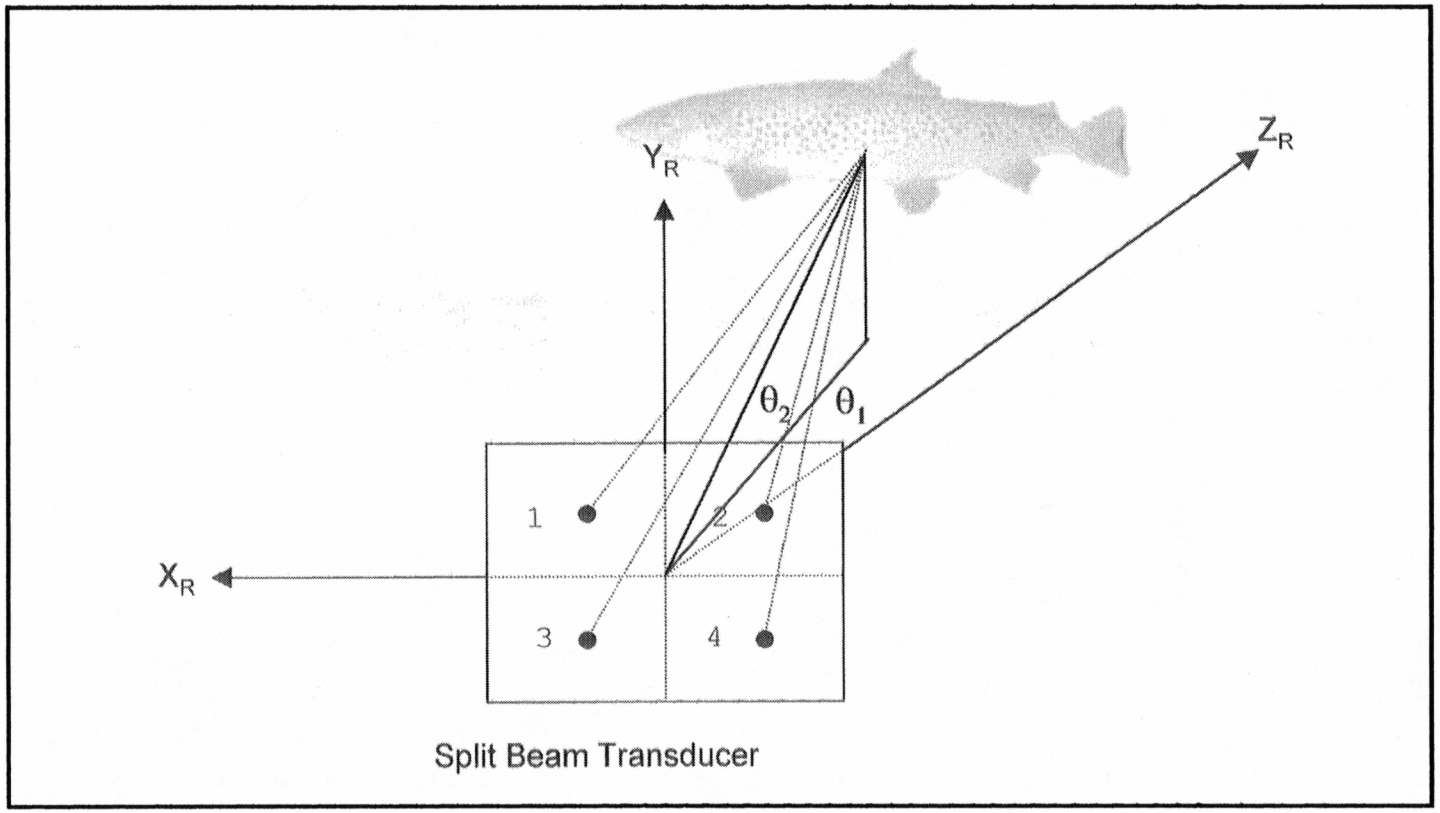

Figure 1. Geometry of the split beam sonar system. Signals received from the four transducer quadrants 1-4 have phase differences which determine the angles θ_1 and θ_2 of the target direction.

to determine the direction of arrival of the pulse. The phase error due to noise can be improved by using a filter to reduce the amount of noise present in the incident signal at each receiver before making the phase measurement. Range difference and/or SNR threshold criteria are used to discriminate between the various phase wrap ambiguities.

2.1.2 Sonar Transducer Beam Pattern

The transducers used in split beam sonar systems are often constructed as an array of individual elements. In a typical transducer each element consists of four ceramic tubes with steel head and tail masses which are designed to ensure efficient transfer of energy into the water. The ceramic tubes are held together by a prestressing bolt. A low density backing material ensures that most of the acoustic energy is transmitted in the forward direction into the water. This type of transducer is reversible, it may be used either to transmit or receive sound waves [MacLennan et al., 1992]. The simulated transducer is modeled as a rectangular array with M = 32 elements in the X_R direction and N = 32 elements in the Y_R direction, where X_R and Y_R are the x and y river coordinate directions discussed later. The modeled elements of the transducer array are separated by $d_1, d_2 = \frac{\lambda}{2}$ meters. An analytic beam pattern function is used to calculate the beam pattern [Skolnik 1962].

$$b(\theta_1, \theta_2) = \frac{\sin(\frac{m\pi d_1}{\lambda} \sin\theta_1)}{m \sin(\frac{\pi d_1}{\lambda} \sin\theta_1)} \cdot \frac{\sin(\frac{n\pi d_2}{\lambda} \sin\theta_2)}{n \sin(\frac{\pi d_2}{\lambda} \sin\theta_2)} \tag{1}$$

Where $b(\theta_1, \theta_2)$ is the two-dimensional gain, m and n are the number of individual elements in the X_R and Y_R directions, d_1 and d_2 are the separation between array elements in the X_R and Y_R directions, λ is the acoustic wavelength, θ_1 is the off-axis angle in the X_R-Z_R plane and θ_2 is the off-axis angle in the Y_R-Z_R plane. The beam

pattern of the entire array is calculated on transmission, and the beam pattern of each of the four quadrants is used for reception. Because the transducer modeled is symmetrical, the individual receivers have $\frac{M}{2}$ elements in the X_R and $\frac{N}{2}$ elements in the Y_R directions.

2.1.3 Path Length Differences and Phase Wrap

The electrical phase is measured at each receiver. The measured phase can be transformed to a path length to the target by:

$$D_{path} = \lambda(\frac{\phi}{2\pi}) \tag{2}$$

where D_{path} is the path length, λ is the acoustic wavelength of the signal, and ϕ is the measured phase. Using the calculated path length, the difference in path length between each receiver can be calculated. The path length differences allow the angle of arrival of the wavefront to be calculated in two dimensions. Since the phase returned is inherently modulo 2π, the path length is modulo λ. Figure 2 shows how the phase wraps for phases greater than $\pm\pi$ with respect to location in the beam. This phase ambiguity causes an ambiguity in the calculation of the direction of arrival of the pulse. The ambiguity arises because a phase ϕ corresponds to $n = \frac{a}{\lambda}$ possible locations, where a is the receiver quadrant center-to-center separation and λ is the acoustic wavelength. The phase ambiguity can be removed by using range difference and echo level thresholding techniques. Another problem associated with phase wrap occurs when the phase measured by the first receiver wraps before the phase measured on the second receiver. Figure 3 shows how the phase changes for two receivers separated by $a = 10$ cm as a target fish moves across the transducer beam.

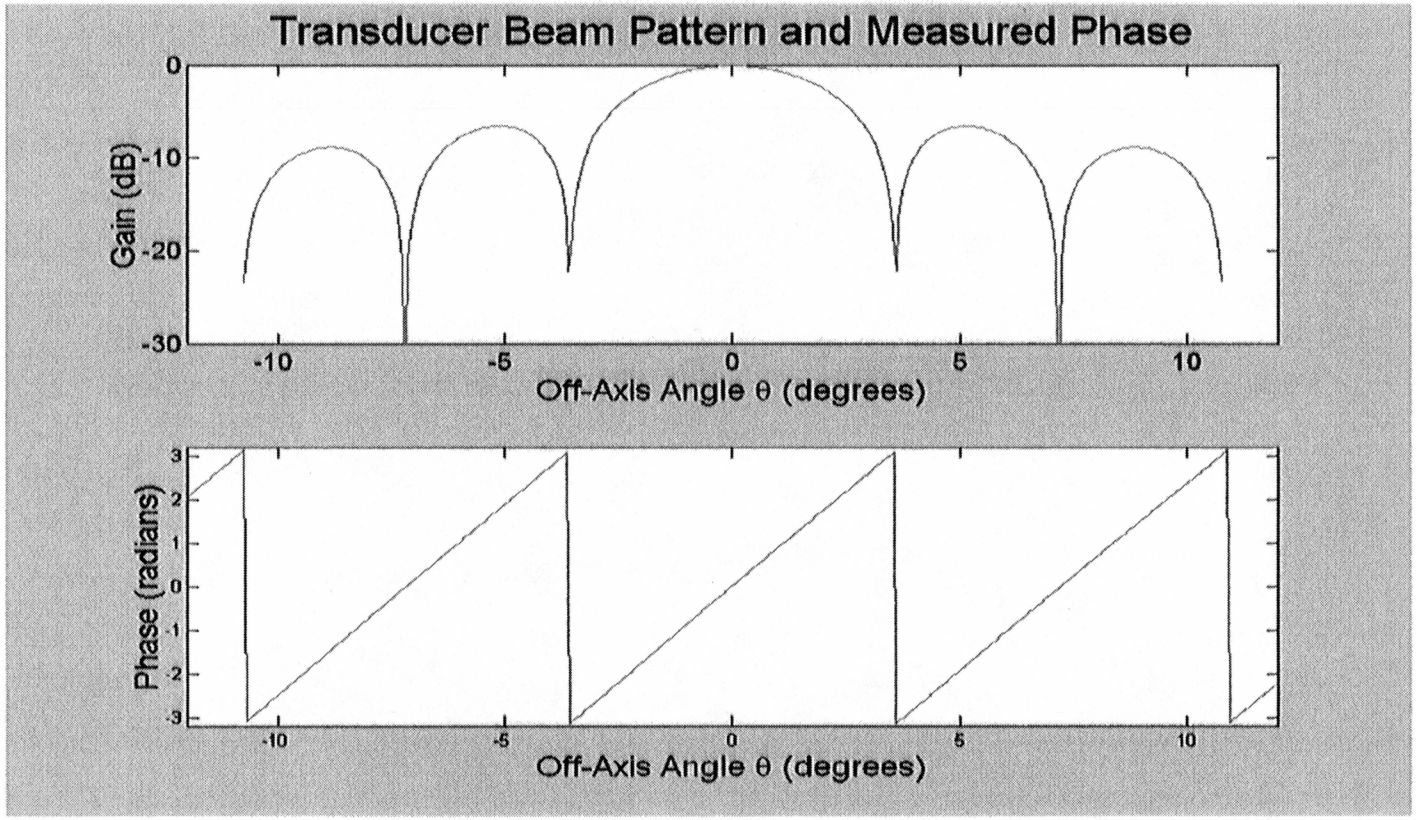

Figure 2. Beam pattern and phase wrap. As the fish moves through the beam of the transducer, the path length difference changes continuously, but the measured phase wraps when the phase exceeds $\pm\pi$. For a rectangular array, the first phase wrap occurs at the same location as the first sidelobe of the transducer.

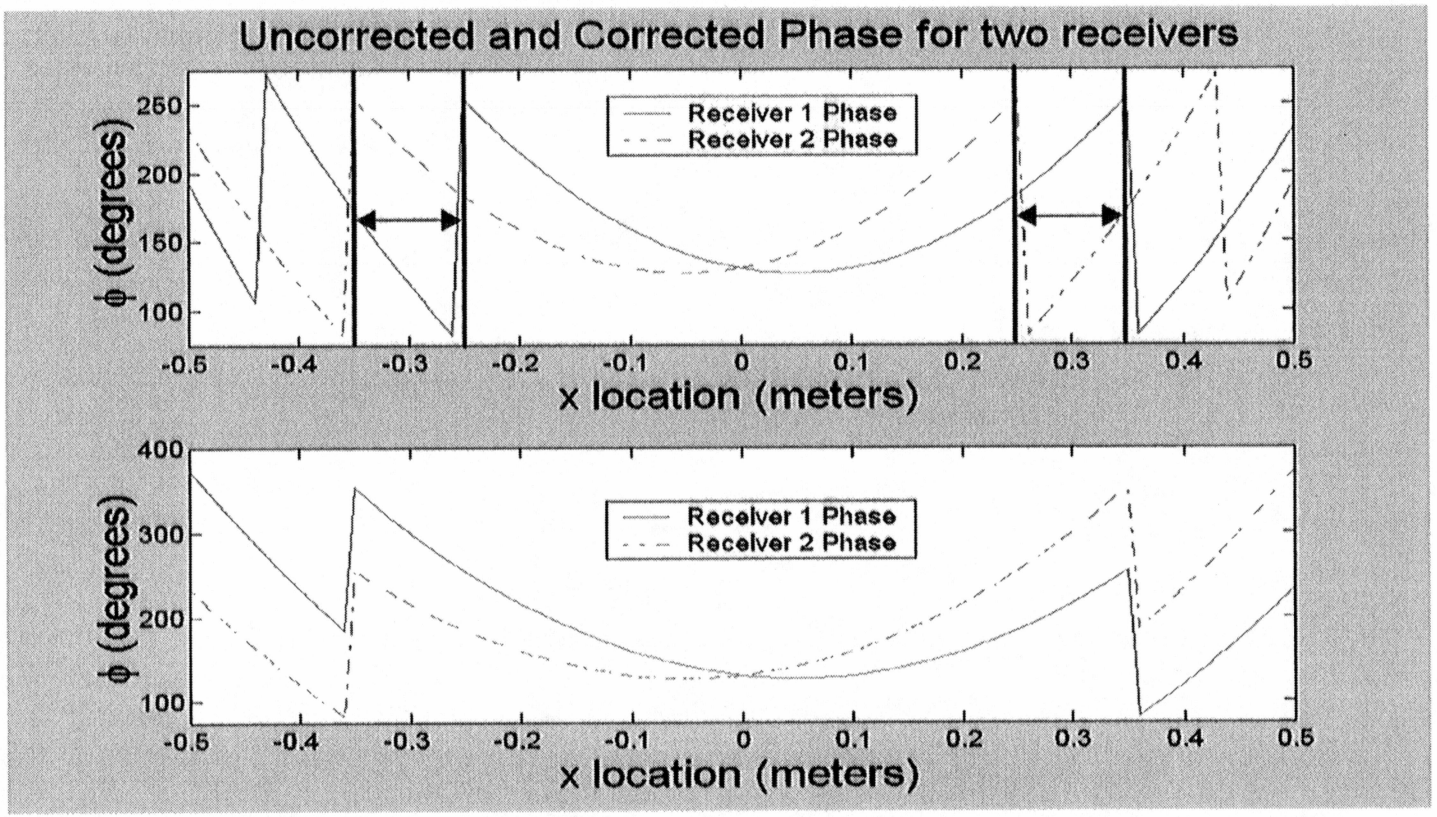

Figure 3. Phase "lead" on two receivers. A discontinuity occurs when the phase measured on one receiver wraps before the phase measured on the second receiver. This is corrected by noting which side of the beam the fish is on and adding the appropriate offset.

Depending on which side of the beam the fish is on, one phase will always "lead" the other. The discontinuity due to phase "lead" can be corrected by noting which side of the beam the fish is on and adding 180 degrees of phase to the signal that is lagging. Adding this phase offset ensures that the difference between the received phases do not have errors due to phase wrap.

Using the time delay of the returned echo, the range to the fish can be estimated for each receiver.

$$R_f = \frac{c\,t_d}{2} \tag{3}$$

where R_f is the range to the fish, c is the speed of sound, and t_d is the time delay of the pulse. These ranges are used to calculate a fish location estimate. The estimated fish location is then used to determine which phase wrap the fish is in. The accuracy of the time delay measurement is limited by the accuracy of the pulse arrival time measurement. Since the pulse is modified by transmission through the river, the shape and magnitude of the pulse can be changed. Therefore, the exact arrival time is difficult to measure. Noise in the sonar system makes calculation of pulse arrival time very difficult when the signal to noise ratio is less than 3 dB. In these cases, the phase wrap determination can fail, leading to large errors in the fish location estimate. When the signal to noise ratio is greater than 3 dB, the phase wrap can be determined with sufficient accuracy to remove the phase wrap ambiguity. Another technique for removing the phase wrap using the echo level exists [MacLennan et al., 1992]. If the fish is modeled as an isotropic reflector, then we can determine which lobe of the beam the fish is in by its echo level. If the transducer used is a linear (or rectangular) array, then the first null in the beam pattern will occur at the same point as the first phase wrap (Figure 2).

A well designed transducer will have the level of the sidelobes well below the level of the main lobe. If this is the case, then the phase wrap ambiguity can be eliminated by rejecting all echoes below some threshold. An ideal transducer would put the sidelobe levels below the receiver threshold so that the only returns received were in the main beam of the transducer. There is a problem with using this method to remove the phase ambiguity. A fish is not an isotropic reflector, in fact, the target strength of a fish can vary by as much as 30 dB depending on the orientation of the fish in the beam. If the echo level is the only method used to determine whether or not the phase is wrapped, then echoes where the fish is in a low target strength orientation can be mistaken for echoes returned from a sidelobe.

2.1.4 Sonar Pulse Model

The sonar pulse incident on the receiver is modeled as a finite duration cosine pulse with finite rise and fall times. The cosine pulse rise and fall are modeled as a modulated half-period cosine wave on either side of a modulated rectangular pulse [Pham 1999]. Figure 4 shows a 120 kHz noise-free pulse with a pulse duration of 66.6 μs, rise and fall times of 41.6 μs and a sampling frequency of 1.2 MHz. Where the pulse duration T_P is defined as the pulse period where the amplitude of the pulse is at 100% of it's peak value, T_R is the time taken for the pulse to pass from 0% to 100% of it's peak value or from 100% to 0% of it's peak value and T_D is the time from the initial transmission of the pulse to pulse reception.

Reverberation and background noise are modeled together as Gaussian random noise.

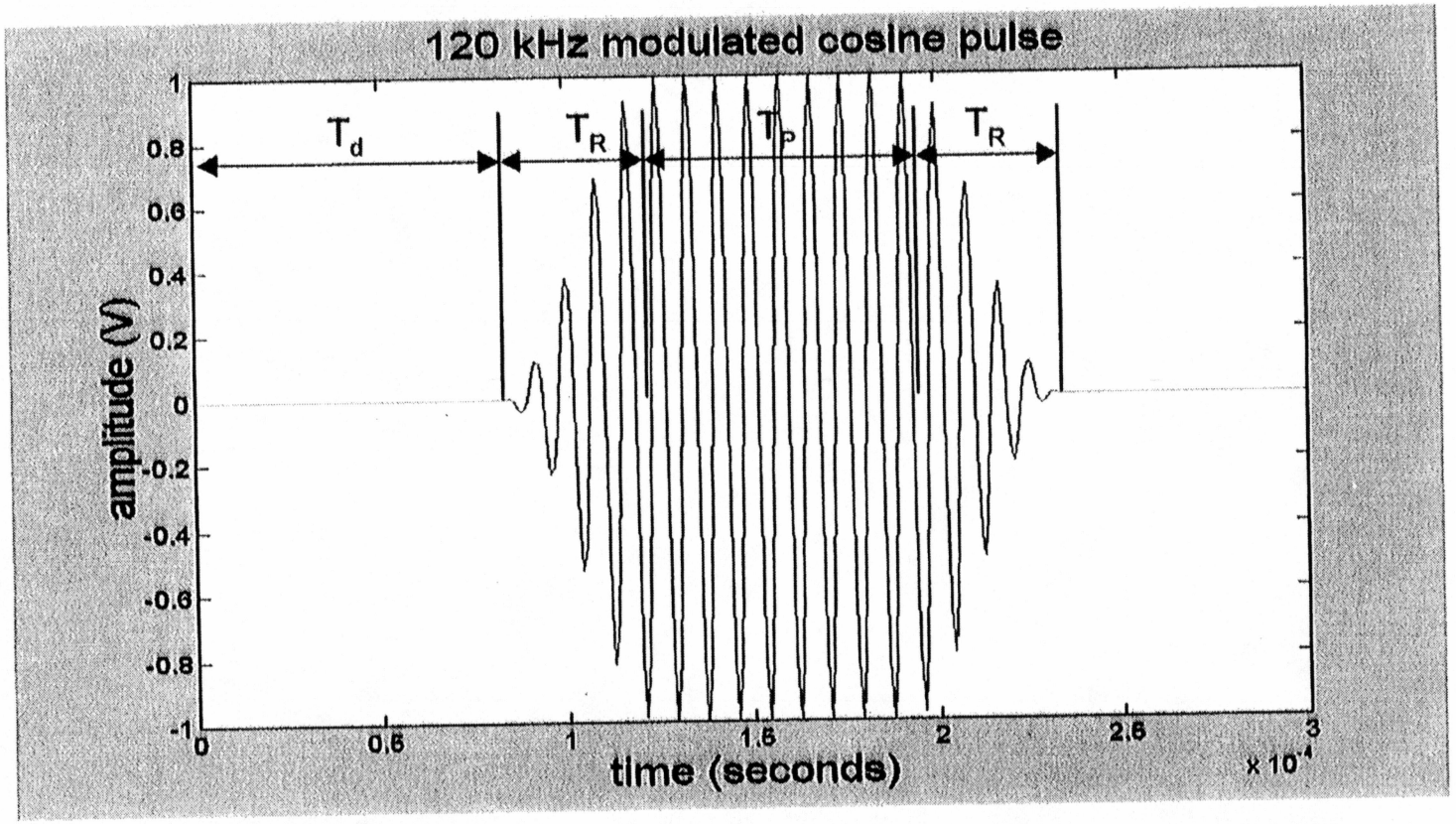

Figure 4. Example of a simulated 120 kHz sonar pulse. The parameters of the pulse are Amplitude = 1 Volt, T_P = 66.6 μs, T_R = 41.6 μs, T_D = 83.3 μs, f_s = 1.2 MHz, ϕ = 0 degrees.

Noise is modeled as an ergodic Gaussian random process [Carlson 1986] with zero mean and standard deviation:

$$\sigma_n = \frac{A}{\sqrt{2SNR}} \tag{4}$$

Where A is the maximum signal amplitude and SNR is the signal to noise ratio of the received pulse. Figure 5 shows an unfiltered pulse with same parameters, but with a signal to noise ratio of 5 dB. We have used a bandpass filter to reduce the noise in the received signal. A rudimentary adaptive filter was developed but was not pursued because of time constraints. Instead, a simple FIR (Finite Impulse Response) band-pass filter is used to reduce noise in the received signal. Every filter has an intrinsic amplitude and phase response associated with it. In general, if the phase response of the filter is not corrected, then the phase values of the received signal will be changed and the original received phase will be lost. The calculation of angle of arrival relies on the relative phase measured at each receiver. Since this is the case, the phase introduced by filtering will cancel out when the phase differences are calculated. The demodulated sonar pulse is also filtered in the receiver model. A FIR low-pass filter is applied to the demodulated pulse, providing noise rejection. Noise in the demodulated pulse is of critical importance to the calculation of fish location. The range to each receiver is calculated from the pulse delay of the demodulated pulse at each receiver. If the pulse is too noisy to give a good estimate of range, then the location estimate made from these ranges will be inaccurate and wrong phase wrap ambiguity will be chosen. Appendix provides a discussion of the filter coefficients used in the low-pass and band-pass FIR filters. The pulse carrier frequency used in most commercial riverine split beam sonar systems ranges from about 100 kHz to about 420 kHz.

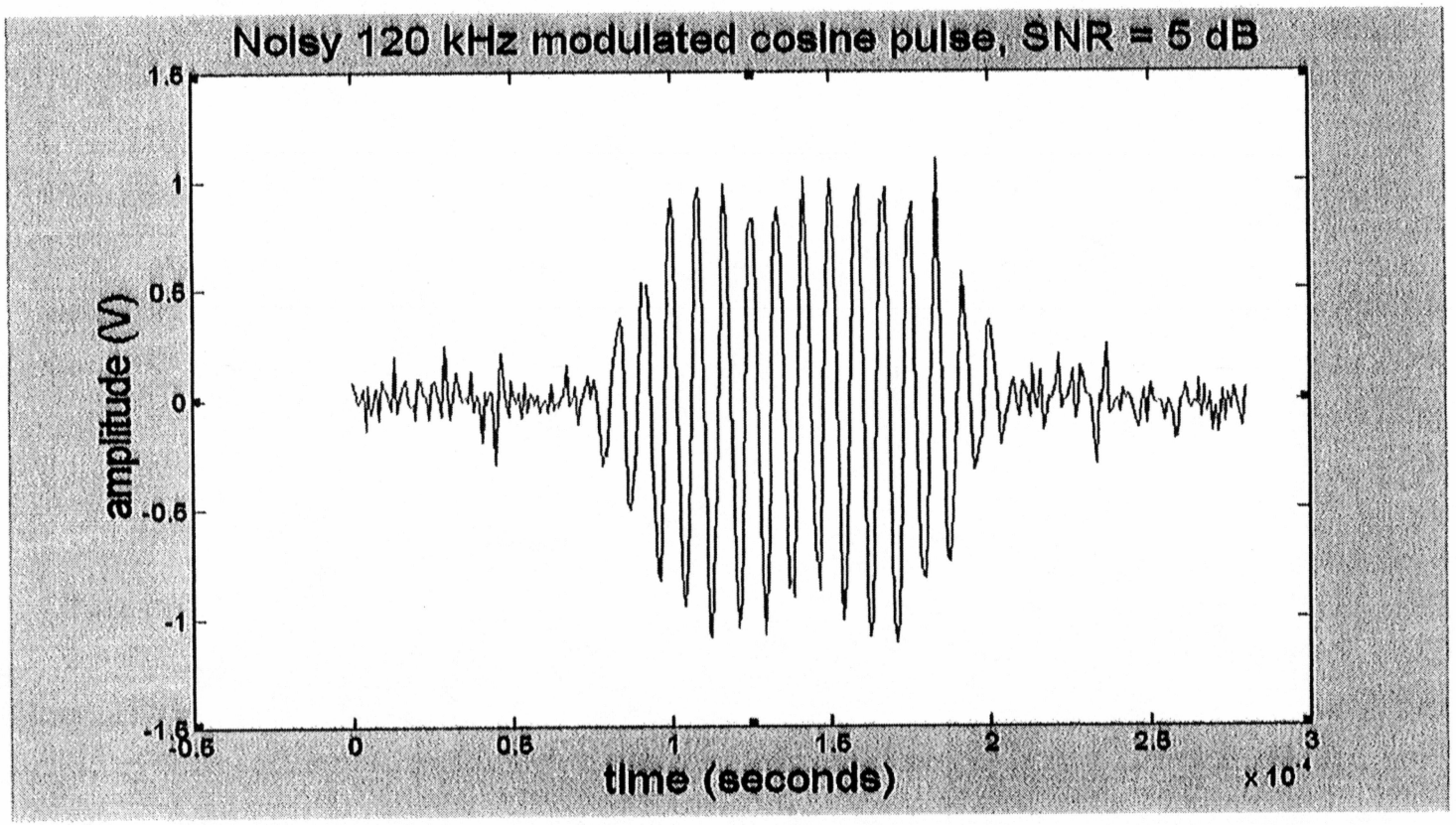

Figure 5. Example of a simulated noisy 120 kHz sonar pulse. The parameters of the pulse are Amplitude = 1 Volt, T_P = 66.6 μs, T_R = 41.6 μs, T_D = 83.3 μs, f_s = 1.2 MHz, ϕ = 0 degrees, SNR = 5 dB

The choice of carrier frequency affects the attenuation of the signal in the water and the target strength of the fish. The choice of carrier frequency is based on several factors including the size of the fish, the range and angular resolution required and the attenuation level allowed (based on the signal to noise ratio and the maximum expected range of the fish).

The sampling frequency of the receiver analog to digital converter is important in the split beam system. It directly affects the quality of the fish location estimate. When noise is present in the system, low sampling frequencies can lead to poor phase measurements. Without filtering of the modulated pulse, we have observed that a sampling frequency of approximately $f_s \approx 10 f_c$ is required for accurate phase and range measurements, where f_s is the sampling frequency and f_c is the carrier frequency. If the received, modulated pulse is filtered, then $f_s \approx 5 f_c$ is adequate. Choosing higher sampling frequencies minimizes these errors.

The duration of the sonar pulse affects the accuracy of the measured phase. Phase is calculated by the in-phase/quadrature method [Carlson 1986]. This method averages over the pulse duration. Therefore a longer pulse provides more averaging and thus more noise reduction. The trade-off is in the system resolution. The resolution of a sonar system is defined as [MacLennan et al., 1992]:

$$x_{min} = \frac{c\tau}{2} \tag{5}$$

Where x_{min} is the minimum distance for two objects to be separated and still be resolved as discrete objects, τ is the pulse duration, and c is the speed of sound in water. Typical pulse durations in commercial split beam sonar systems range from about 0.1 ms to 1 ms, corresponding to a resolution of 7.5 cm and 75 cm respectively.

The amplitude of the transmitted pulse is arbitrary in this model. The parameter of interest is the signal to noise ratio, and not the absolute amplitude of the pulse. The noise level is calculated relative to the amplitude of the pulse. In this thesis the received pulse is modeled with unit amplitude.

The rise and fall times of the pulse are a function of the fish flesh and swim bladder interfaces. The values for these parameters are not modeled and a single, constant value of 0.1 ms is assumed for all of the simulations. Because the rise time of the pulse directly affects the measured pulse delay, changes in the rise time of the received pulse will influence the calculated range. These errors will make it more difficult to determine the phase wrap of the received signal and could result in phase wrap errors in the fish location estimate.

2.1.5 Sonar Equation and Calculation of Signal to Noise ratio (SNR)

The signal to noise ratio of the pulse is dependent on range, transducer beam pattern, signal attenuation, fish target strength, reverberation level and background noise. Receiver noise is neglected in this treatment, since the receiver noise level is typically much lower than that of the background river noise and reverberation. All of the calculations in this treatment assume that the fish is in the far field of the transducer. The far field range can be estimated using the following equation [MacLennan et al., 1992].

$$R_b = \frac{a^2}{\lambda} \tag{6}$$

Where R_b is the approximate range to the far field condition, a is the transducer width or height, and λ is the acoustic wavelength. If the array is a rectangular then the larger of the two dimensions should be used to calculate the far field range.

The signal to noise ratio is calculated by: [MacLennan et al., 1992]

$$\mathrm{SNR}_{rcvd} = \mathrm{SNR}_{ref} + \mathrm{TL} + \mathrm{BF} + \mathrm{TS} \tag{7}$$

where:

SNR_{rcvd} = Received SNR Level (dB)

SNR_{ref} = Reference SNR Level (dB)

TL = Transmission Loss (dB)

BF = Beam Factor (dB)

TS = Target Strength (dB)

SNR_{ref} is the SNR of a received pulse with a target strength of 0 dB located at a unit distance from the transducer (TL = 0 dB and BF = 0 dB). The transmission loss calculation assumes that the wave is far away from the transducer and can be modeled as a spherical wave. It includes the effects of spreading loss and attenuation. The expression for the one-way spreading loss is given by:

$$\mathrm{loss} = 20 \log \frac{R_f}{R_{ref}} \tag{8}$$

Where R_f is the range to the target fish and R_{ref} is the reference range (1 m). The attenuation is given by a empirical equation based on the frequency of the transmitted pulse, temperature of the water and the salinity of the water [Urick 1983]. The beam factor is given by the equation 1. The target strength of the fish is a function of the orientation of the fish with respect to the incident wave normal vector $\hat{k}$ as shown in figure 6 and is defined by the angles θ_k and ϕ_k. The return from the fish is calculated at the point on the fish where the incident wave falls normally. Target strength is modeled using previous results which indicate that for fish with swim bladders

(salmon have a swim bladder), most of the target strength contribution comes from the swim bladder [Sonwalker et al., 1999]. The expression for target strength is given by:

$$TS = 10 \log \frac{R_1 R_2}{4} \tag{9}$$

where:

$$R_1 R_2 = \frac{A^2 B^2 C^2}{[(A^2 \cos(\phi_k)^2 + B^2 \sin(\phi_k)^2) \sin(\theta_k)^2 + C^2 \cos(\theta_k)^2]^2} \tag{10}$$

A, B and C are the ellipsoidal axes of the simulated fish's swim bladder. A is one half of the length of the swim bladder in the direction from fillet to fillet, B is one half the length of the swim bladder in the direction from from belly to dorsal fin and C is one half the length of the swim bladder in the direction from nose to tail of the fish. θ_k and ϕ_k are the incidence angles shown in figure 6. The noise level is calculated using the modeled received SNR level and the amplitude of the transmitted pulse. The noise level is:

$$\mathrm{N}_{dB} = 0 - \mathrm{SNR}_{dB} \tag{11}$$

The equation above assumes that the unit amplitude for the transmitted pulse as described in Section 2.1.4.

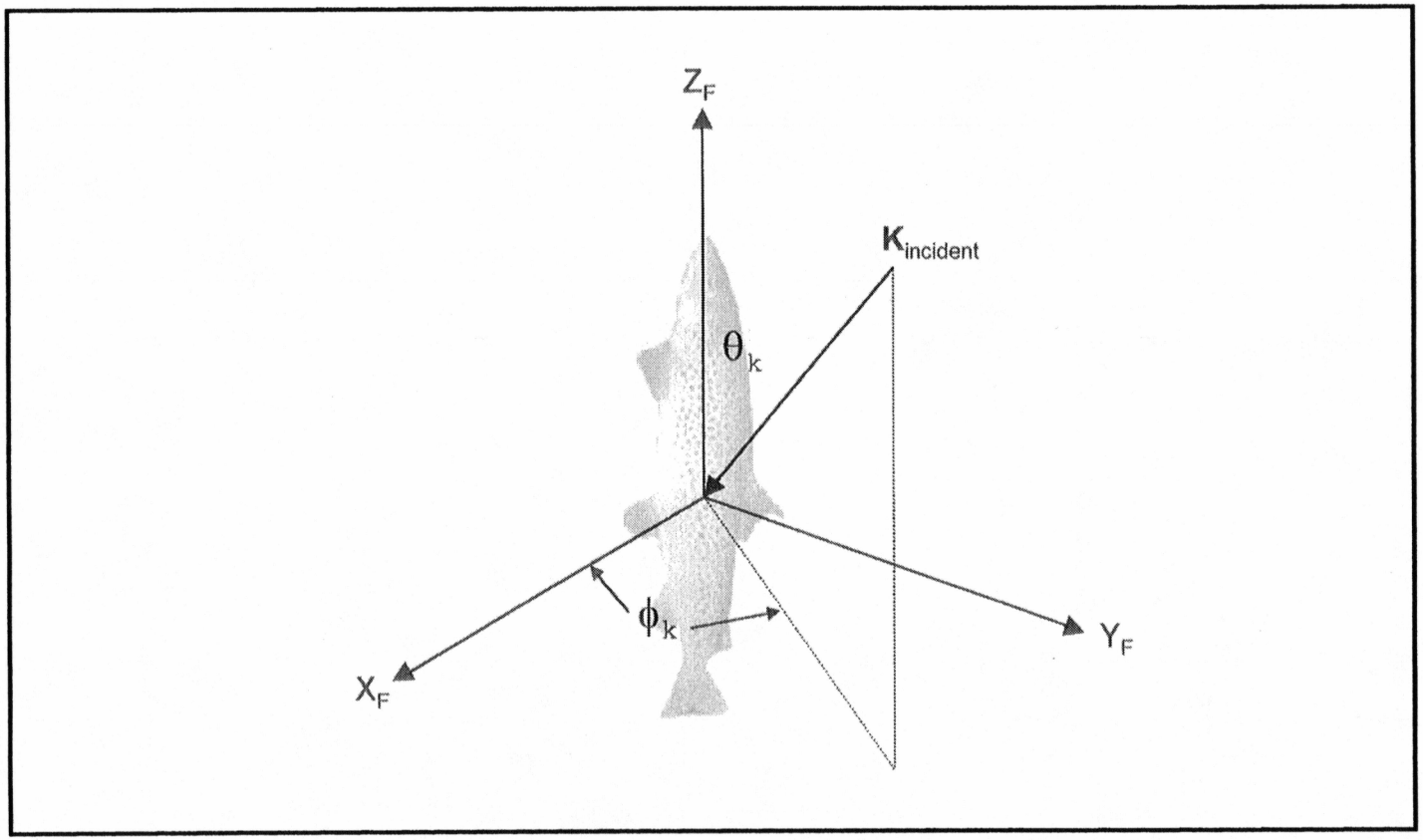

Figure 6. Angles of incidence θ_k and ϕ_k. Target strength is a function of incidence angles θ_k, ϕ_k and is calculated using a recently developed model. [Sonwalker et. al. 1999]

2.2 Simulation Model

The computer simulation performed in this thesis models a split beam system and measures the uncertainty in fish location under noisy conditions. To perform this, Matlab m-files were written to model different parts of the sonar system, simulate the received pulse and implement various signal processing and analysis techniques.

Figure 7 is a description of the pulse parameter calculations. These parameters are used to simulate a received sonar pulse for a fish with a given location and orientation. The user is required to input values for fish location [x y z], reference signal to noise ratio SNR_{ref}, fish orientation [θ_v ϕ_h θ_{roll}], fish size [L W H], number of transducer elements (M, N) and transducer element separation (d_1, d_2). The fish location is used to calculate the path length to the fish from each receiver quadrant. The one-way transmission loss due to spherical spreading is calculated by applying equation 8 to the fish location. The fish target strength is calculated by equation 9 and is a function of the fish orientation and size. The transducer beam factor is calculated by equation 1 and is a function of the number of transducer array elements and the separation between those elements. The sonar equation (equation 7) is applied using the transmission loss (TL), target strength (TS) and beam factor (BF) results. The phase [ϕ_1 - ϕ_4] and time delays [τ_1 - τ_4] are calculated based on the distance to the fish using equations 16 and 17.

2.2.1 Coordinate system and fish orientation

The fish location in this model is described using both Cartesian and spherical coordinates. A vector [x, y, z] describes the fish location in Cartesian coordinates, while a vector [R, θ, ϕ] describes the fish location in spherical coordinates.

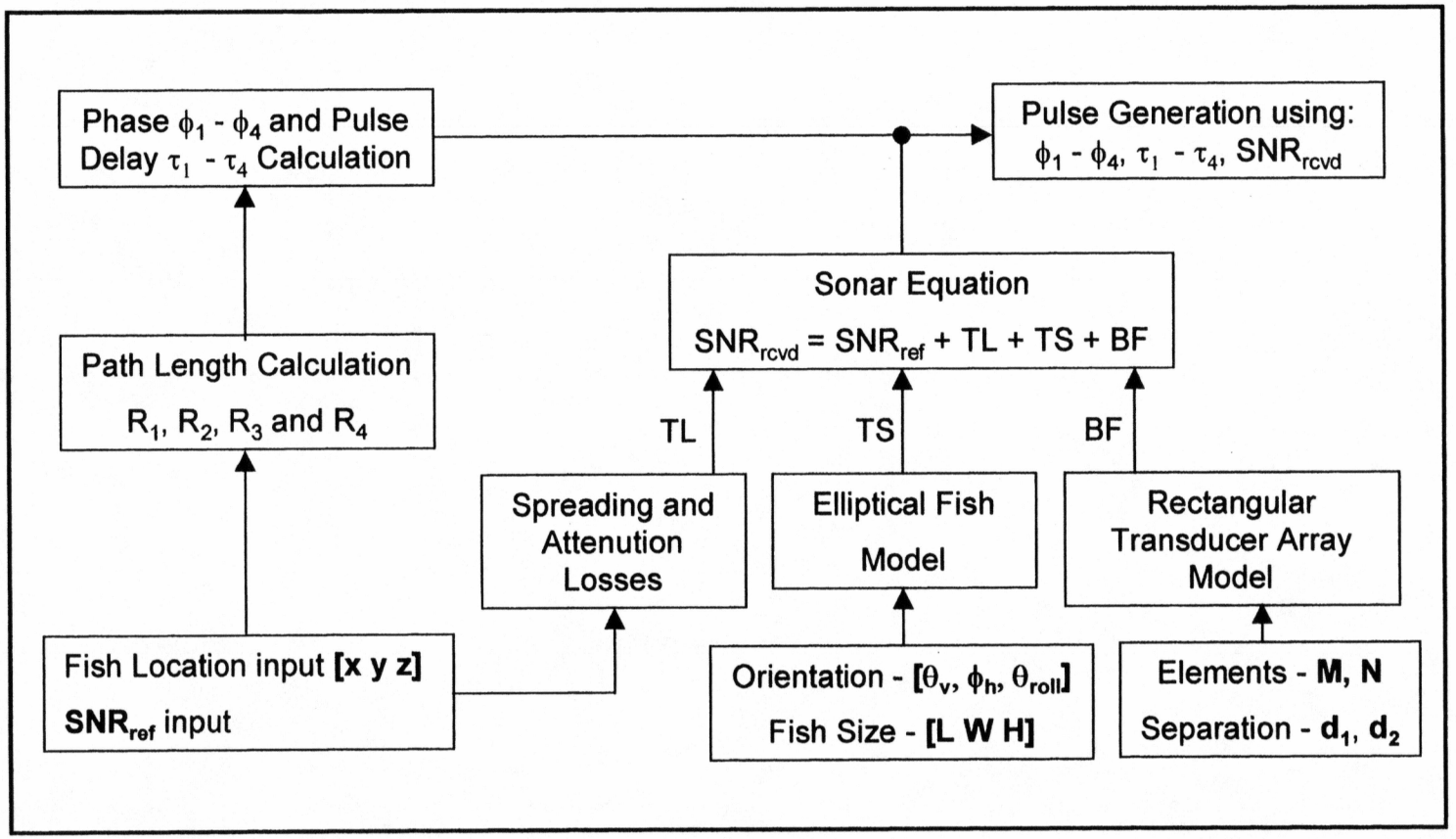

Figure 7. Pulse parameter calculation flow diagram. This diagram shows the steps in producing the parameters for a modeled pulse. **Bold** type indicates user specfiied inputs.

The angle of arrival measurement used in this thesis is described in terms of two angles, θ_1 and θ_2. These are the left/right and up/down angles off of the acoustic axis. The simulations in this thesis are performed primarily in Cartesian coordinates, where the angles θ_1 and θ_2 can be related to [x y z] by:

$$\theta_1 = \arctan \frac{x}{z} \tag{12}$$

$$\theta_2 = \arctan \frac{y}{z} \tag{13}$$

The calculated fish location estimates are converted from Cartesian coordinates to θ_1 and θ_2 for the figures in the thesis. The angles θ_1 and θ_2 can be related to the spherical angles θ and ϕ by an approximation [Ehrenberg 2000]:
If we assume that R $\gg$ x and R $\gg$ y, then

$$\theta \approx \arcsin \sqrt{\tan^2 \theta_1 + \tan^2 \theta_2} \tag{14}$$

$$\phi = \arctan(\frac{\tan \theta_1}{\tan \theta_2}) \tag{15}$$

Where θ is the spherical angle made between the vector [x y z] and the z-axis, and ϕ is the counterclockwise angle of [x y z] projected into the xy plane measured from the positive x axis. Three different orthogonal coordinate systems are used in the model.

The river, sonar and fish systems are defined as shown in figures 8,9 and 10.

The river coordinate system [X_R Y_R Z_R] is defined with the z-axis perpendicular to the river bank and pointed away from the sonar location. The y-axis is vertically upward, and the x-axis is given by the right hand rule.

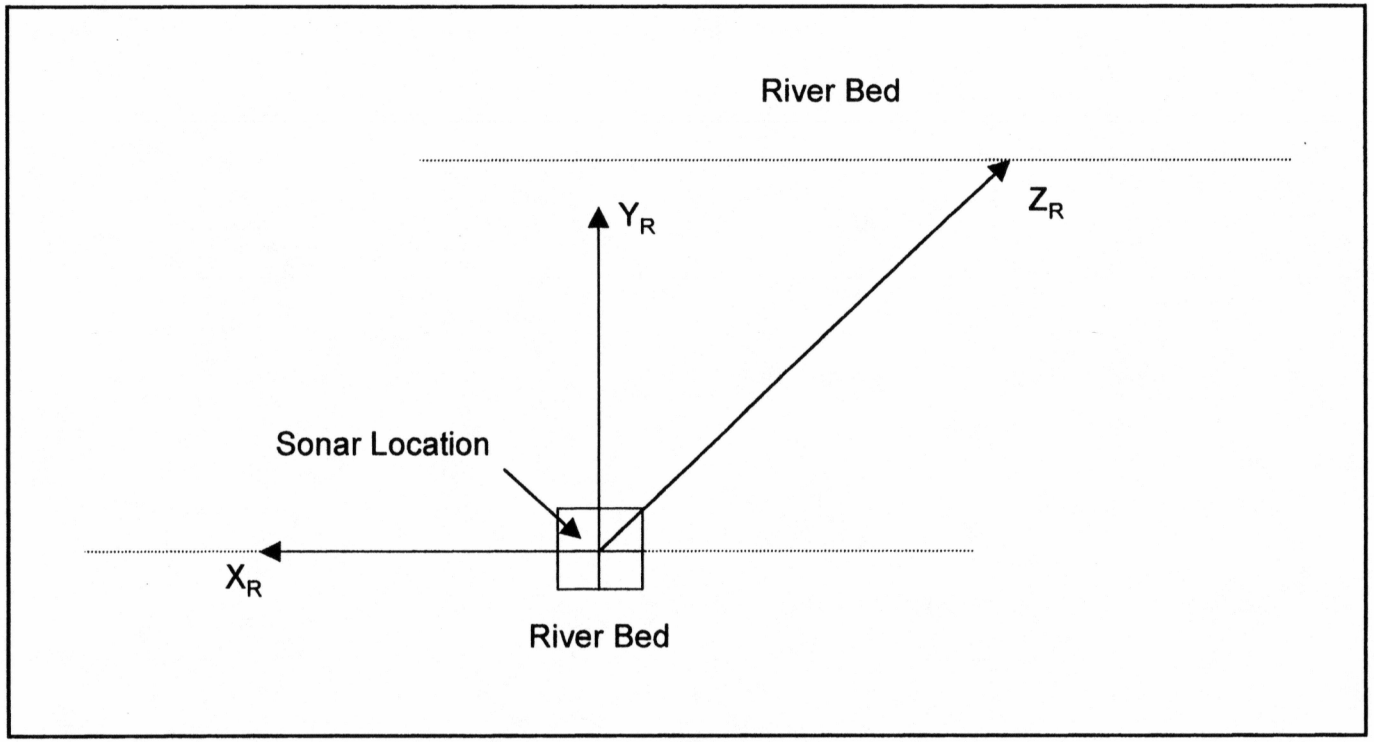

Figure 8. River coordinate system. The Z_R axis is perpendicular to the river bed and points away from the sonar location. Y_R points vertically upward and X_R is given by the right hand rule.

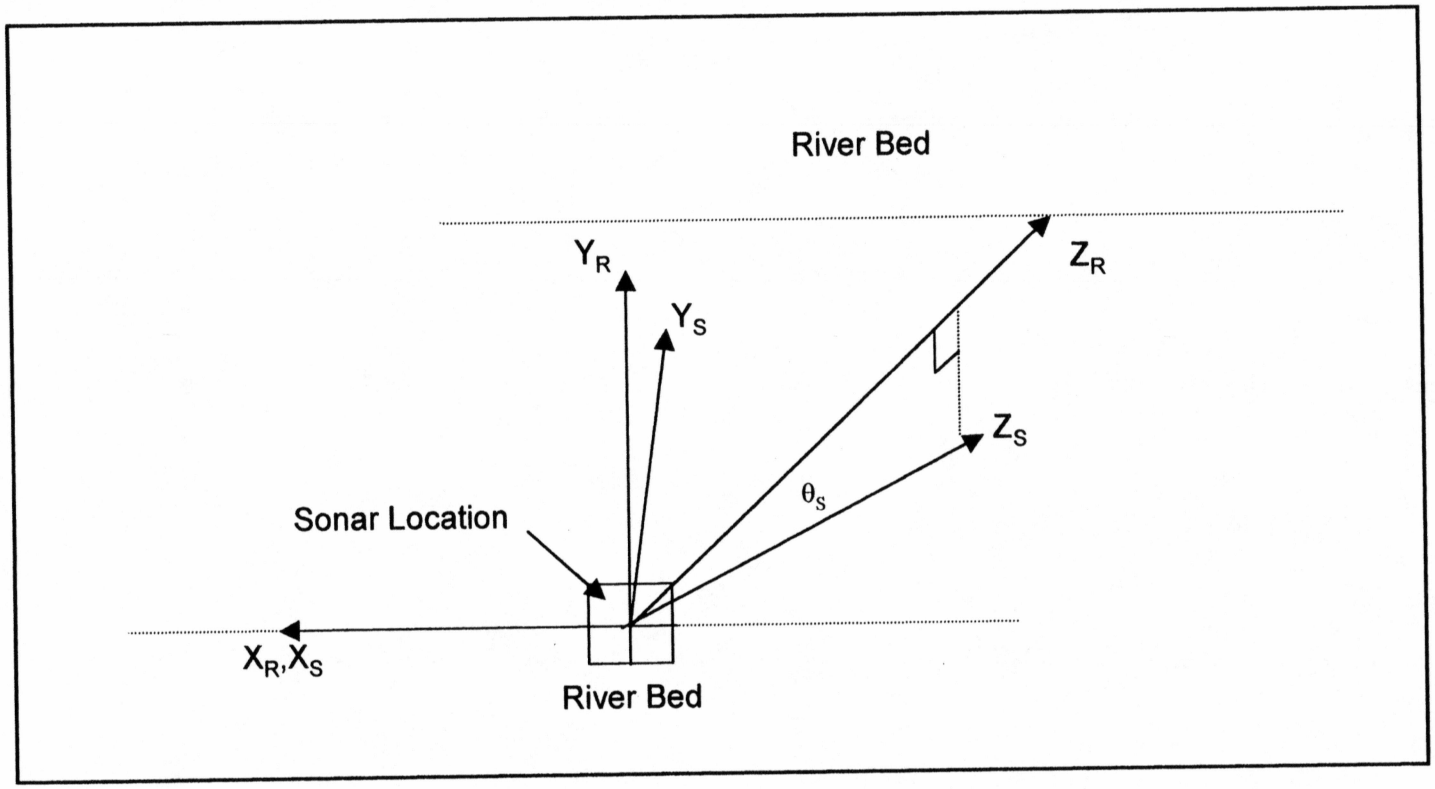

Figure 9. Sonar coordinate system. Z_S is in the direction of the sonar beam axis. Y_S is in the Y_R - Z_R plane perpendicular to Z_S and X_S is given by the right hand rule. θ_S is the angle of tilt in the Y_R - Z_R plane.

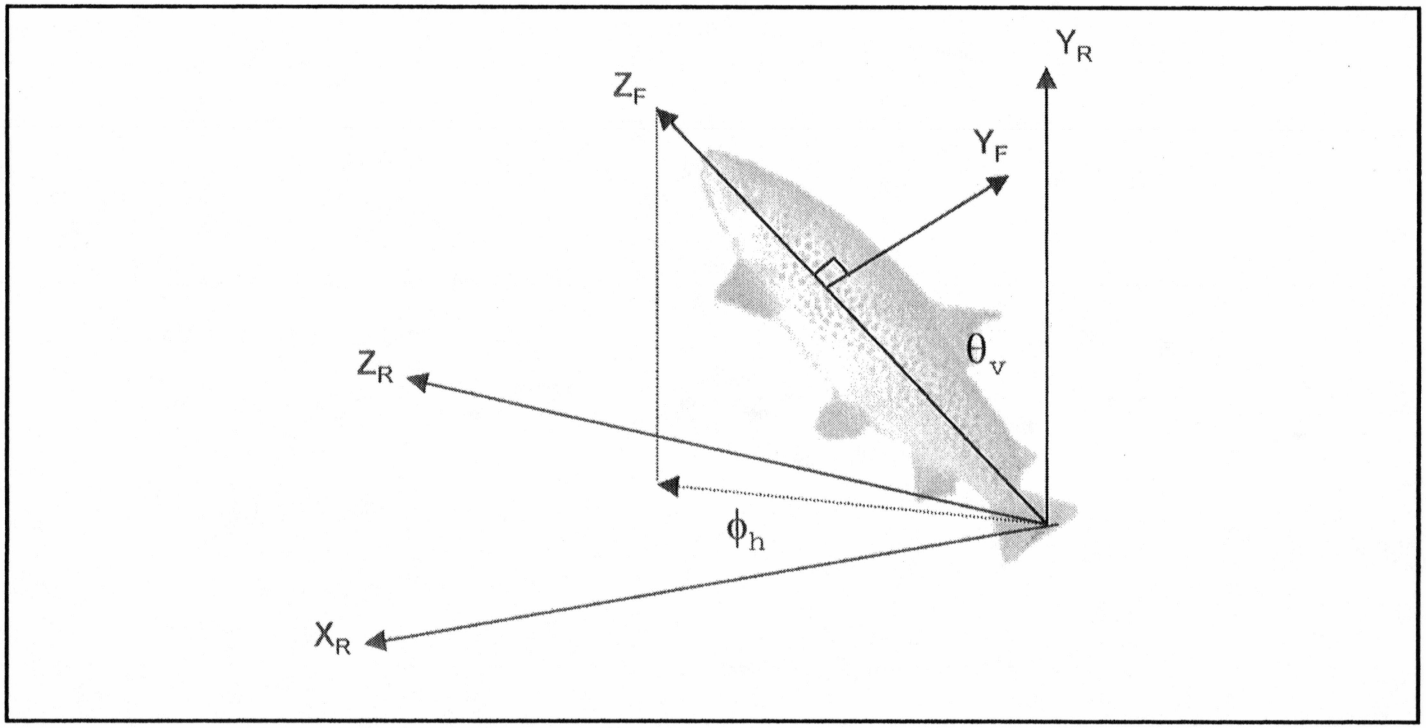

Fish Coordinate System [X_F Y_F Z_F]

Figure 10. Fish coordinate system. The fish coordinate system is defined with Z_F in the direction of the fish tail to head. The Y_F axis is perpendicular to the Z_F axis and in the direction of the dorsal fin, X_F is given by the right hand rule. θ_v and ϕ_h are the spherical angles associated with the fish system. θ_{Roll} (not shown) is the angle of roll about the Z_F axis.

The sonar system is defined to allow the sonar to be tilted downward into the river, as is usually the case. Z_S is in the direction of the sonar beam axis. Y_S is in the $Y_R - Z_R$ plane and perpendicular to Z_S. X_S is given by the right hand rule. The angle θ_s is the angle of tilt of the sonar beam axis in the $Y_R - Z_R$ plane.

The fish coordinate system is defined with Z_F in the direction of the fish tail to head. The Y_F axis is perpendicular to the Z_F axis and in direction of the dorsal fin, and the X_F is given by the right hand rule. The angle θ_v is the spherical angle between the Y_R axis and the Z_F axis. The angle ϕ_h is the angle between the X_R axis and the projection of the Z_F axis into the X_R-Z_R plane. $\theta_r oll$ is the angle of roll about the Z_F axis. The dorsal fin is oriented vertically upward and thus $\theta_r oll$ is equal to zero for all of the simulations in this thesis.

The appendix provides a thorough discussion of the transformations between the coordinate systems.

2.2.2 Path Length Calculation

To measure the uncertainty in the location of fish, a fish is assumed to be located at [x y z] and the path length to the fish is calculated from the center of each receiver to the point on the fish where the incident wave falls normally. The fish is modeled as a point target for the path length calculation. Path lengths are calculated by:

$$D_{path} = \sqrt{(x - x_0)^2 + (y - y_0)^2 + z^2} \tag{16}$$

Where D_{path} is the path length to the receiver, [x y z] is the assumed location of the fish, and x_0 and y_0 are the x and y locations of each receiver, $z_0 = 0$ for the receivers

in this model. The path lengths are converted to phase values by applying:

$$\phi = \text{modulo}(\frac{2\,\pi}{\lambda} D_{path},\, 2\,\pi) \quad \text{(radians)} \tag{17}$$

Where ϕ is the phase of the received pulse and λ is the acoustic wavelength. The path lengths that are calculated are used to produce time delays for the pulse model. These time delays describe the range of the fish. The round trip pulse delay is:

$$t_d = \frac{2\,\mathrm{R}}{c} \quad \text{(seconds)} \tag{18}$$

Where t_d is the time delay in seconds, R is the path length to the receiver, and c is the speed of sound in water. The speed of sound in water is assumed to be 1500 m/s for all of the simulations performed in this thesis.

Figure 11 shows the received pulse generation algorithm. The calculated values for quadrant phase, time delay and SNR_{rcvd} are used to simulate a received sonar pulse using user specified parameters. The pulse carrier frequency f_c, pulse rise/fall time t_r, pulse duration T_p and the pulse sampling frequency f_s are all input by the user. The received pulse at each receiver quadrant is then split into two signals. The first signal is FIR band-pass filtered and used to calculate the received phase. The second signal is demodulated and FIR low-pass filtered. The demodulated signal is used to estimate the time delay in the fish location estimate.

2.2.3 Modeled pulses

A noisy pulse is generated for each of the four receiver quadrants using the time delay t_d and phase ϕ calculated from the known fish location. A constant value of 0.1 ms is assumed for rise/fall time and 1 ms is assumed for the pulse duration.

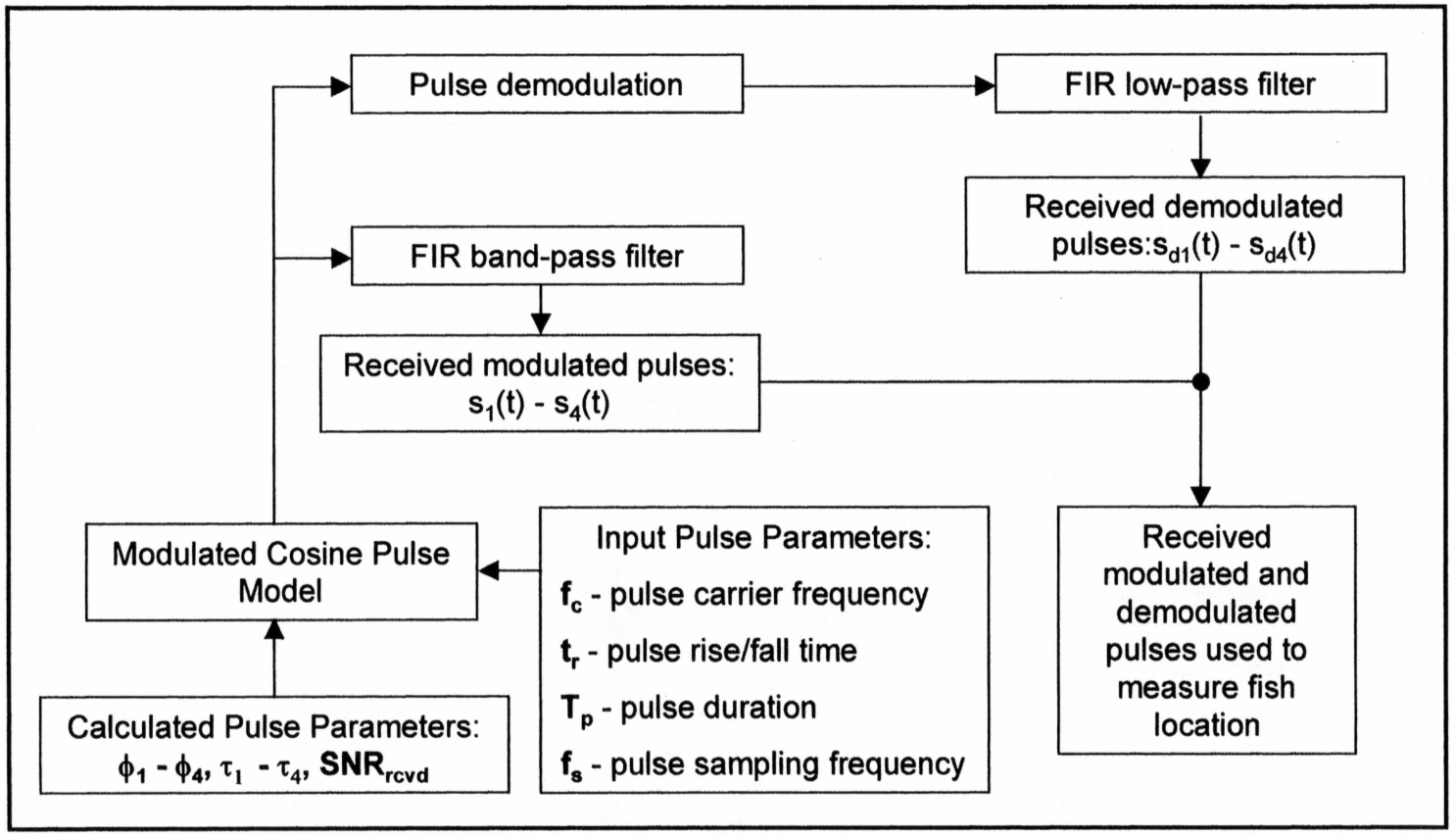

Figure 11. Received pulse generation flow diagram. This diagram shows the steps in producing the modeled pulse incident at each receiver. **Bold** type indicates input parameters.

The four pulses are modulated with a carrier waveform at a frequency of $f_c = 120$ kHz and sampled at a frequency $f_s = 1.2$ MHz. Noise is then added to the pulses using the signal to noise ratio calculated from the fish orientation, fish location, transducer beam factor, and source level. The equation describing the pulse with $T_R = T_F = 0$ is:

$$\mathrm{s(t)} = cos(2\pi f_c(t - t_d) + \phi) + \mathrm{n(t)} \quad t_d \leq t \leq (t_d + T_p) \tag{19}$$

$$\mathrm{s(t)} = \mathrm{n(t)} \quad \text{otherwise} \tag{20}$$

where s(t) is the noisy pulse, n(t) is the Gaussian noise, f_c is the carrier frequency, t_d is the pulse delay, ϕ is the pulse phase, and T_p is the pulse duration (see figure 4).

2.2.4 Range Estimation

The range to the fish from each receiver is estimated using the round trip pulse delay. The pulse delay is measured from the demodulated noisy pulse. Figure 12 shows a demodulated pulse with SNR = 5 dB after FIR-low pass filtering. Two different algorithms were developed to estimate the pulse delay because calculating the range accurately is critical to removing the phase wrap ambiguity. The first algorithm determines a region of silence in the returned echo based on the transmitted pulse width and the number of samples in the returned echo. In this region of silence, the standard deviation of the signal is measured, providing an estimate of the variance of the noise in the signal with time. This standard deviation σ is used to establish a threshold greater than 4σ for the arrival voltage of the returned echo. The choice of 4σ is arbitrary and was chosen because the probability of observing a voltage greater than 4σ is less than 10^{-4} for Gaussian noise.

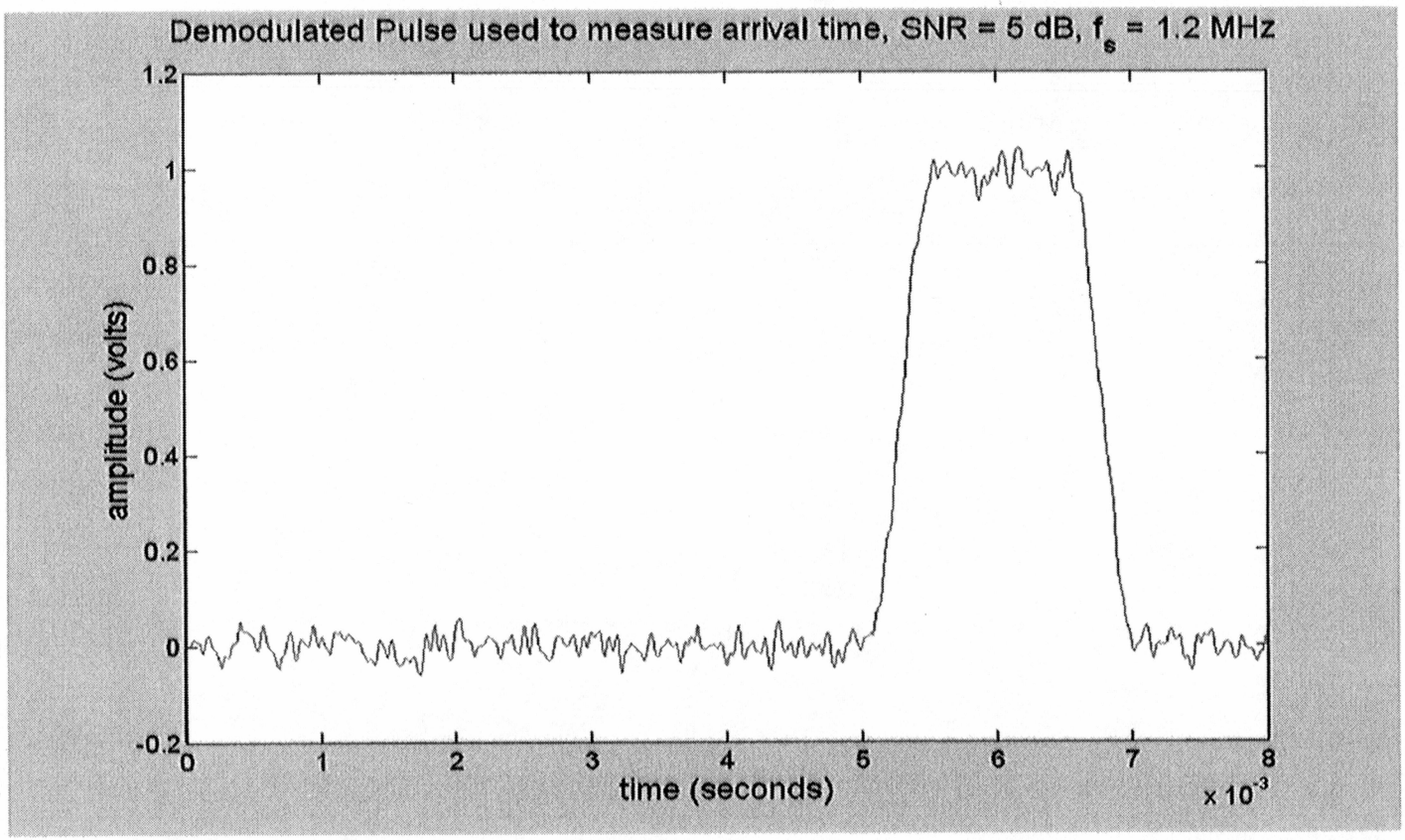

Figure 12. Demodulated pulse used to measure echo arrival time. The pulse has has been FIR low-pass filtered. The standard deviation σ of the noise is measured in the region where no pulse exists. σ is then used to estimate the noise level and choose the first voltage level above the noise as the echo arrival time.

Once the threshold voltage is established, the algorithm looks for the first voltage greater than 4σ which will be the first part of the returned echo. This method of range estimation is dependent on the received signal to noise ratio, thus the higher the signal to noise ratio, the more accurate the fish range estimate. The relative phase of the signal incident on each of the four quadrants is not be affected by this signal to noise ratio dependence.

The second algorithm uses a matched filter to estimate the amplitude of the returned pulse. A matched filter is constructed using the transmitted pulse parameters (Appendix). The filtering operation is performed in the frequency domain to increase speed. Once an estimate of the pulse amplitude has been calculated, an arbitrary level of arrival voltage must be set. The value used in this treatment was 90% of the echo amplitude. This provides a consistent result between all four receivers because the amplitude of the echo on each receiver does not vary significantly.

The first algorithm uses a dynamic estimate of the noise level and is more robust than looking for a fixed voltage. The range to the fish can vary due to the rise time of the pulse. If the rise time of the pulse changes, then the detected arrival of the pulse will also change. If the detection voltage is chosen at a fixed level, then if the rise time increases, error will result in the range estimate because the expected voltage will take longer to arrive. Dynamically changing the arrival voltage using σ allows the algorithm to choose the smallest possible voltage that is above the noise level, minimizing the error in range due to rise time. Neither of these techniques works effectively when the signal to noise ratio is less than 5 dB. More research is required on this topic because of the crucial role it plays in the phase wrap determination.

2.2.5 Phase Estimation

The noisy pulse phase is calculated using the in-phase/quadrature method. Figure 13 shows a block diagram of in-phase/quadrature phase measurement [Carlson 1986]. The phase is calculated by first mixing (multiplying) the pulse with a sine and a cosine waveform of the same frequency as the pulse (f_c). The mean of each waveform is then calculated. The phase of the signal is calculated by:

$$A_i = \text{Mean}[s(t) \times \cos 2\pi f_c t] \tag{21}$$

$$A_q = \text{Mean}[s(t) \times \sin 2\pi f_c t] \tag{22}$$

$$\phi = \arctan \frac{A_q}{A_i} \quad \text{(radians)} \tag{23}$$

where A_i and A_q are the mean of the in-phase and quadrature signal components, f_c is the carrier frequency, s(t) is the received signal, and ϕ is the calculated signal phase. The phase that is calculated using this method is modulo 2π instead of π because the arctan (atan2(A_q,A_i) function in Matlab) function used calculates angles from $-\pi$ to π.

2.2.6 Range and Phase Averaging

Once the ranges and phases have been calculated the half-beams are combined to reduce the noise in the estimates. The half-beam is defined here as the sum of any two adjacent quadrants. Thus a left phase half-beam can be formed by averaging the phase received in quadrants 1 and 3 (see equation 26). The half-beam phase estimates are calculated by averaging in the up/down and left/right directions.

$$\phi_{up} = \frac{\phi_1 + \phi_2}{2} \tag{24}$$

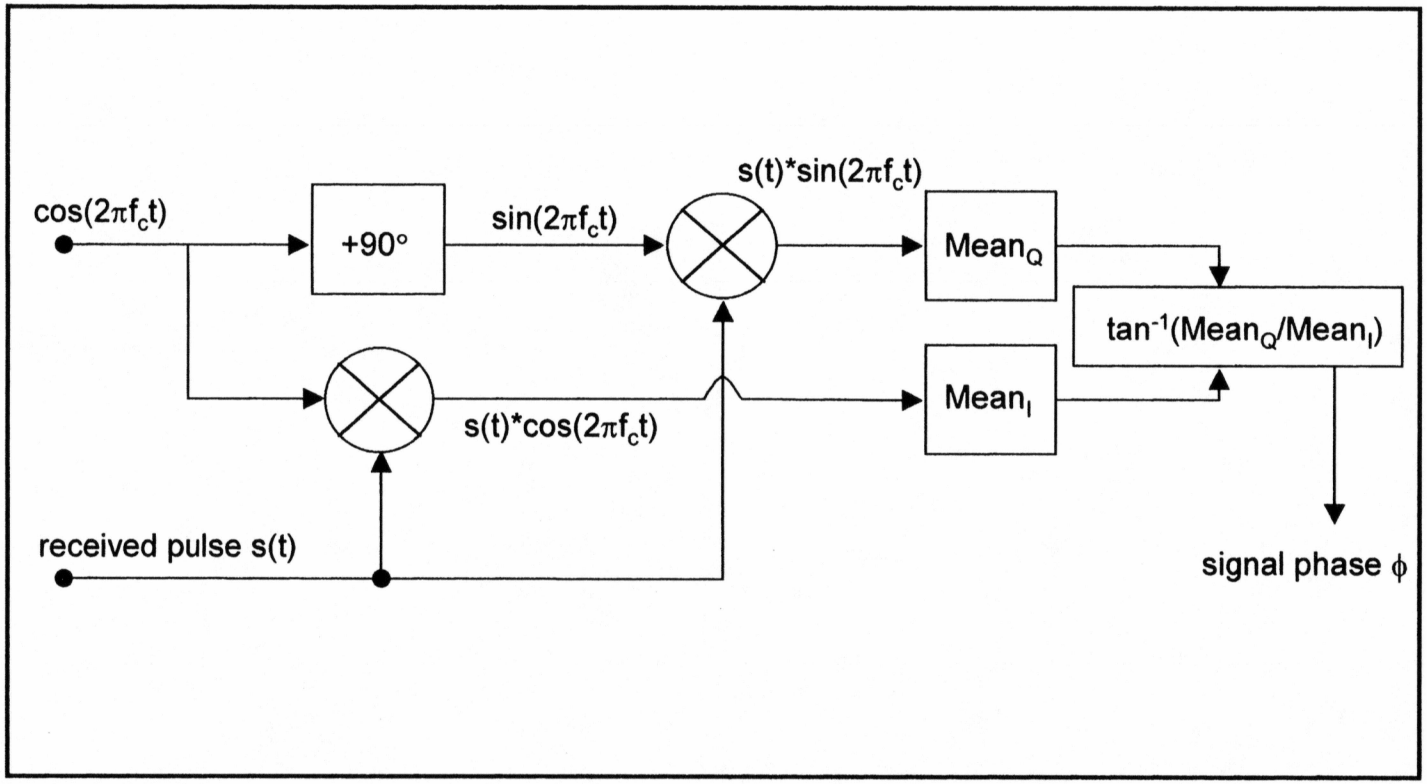

Figure 13. In-phase/Quadrature phase measurement diagram. The input signal s(t) is mixed with sine and cosine waves at the same frequency and the mean of each of these is calculated. An arctan function providing angles from $-\pi$ to $+\pi$ is then used to calculate the phase ϕ.

$$\phi_{down} = \frac{\phi_3 + \phi_4}{2} \tag{25}$$

$$\phi_{left} = \frac{\phi_1 + \phi_3}{2} \tag{26}$$

$$\phi_{right} = \frac{\phi_2 + \phi_4}{2} \tag{27}$$

Where ϕ_{up}, ϕ_{down}, ϕ_{left} and ϕ_{right} denote the up, down, left and right half-beam phases and ϕ_1 - ϕ_4 are the received phase at each transducer quadrant. The same half-beam calculation is performed on the measured range values as well. Averaging is possible because only two receivers are required to calculate the up/down or left/right direction. The averaging operation reduces the noise in the range and phase estimates.

2.2.7 Fish location extraction

Once the ranges and phases have been calculated from the 4 received pulses, the location of the fish can be estimated. The location estimate from the calculated ranges uses the range differences from the transducer half-beams. The [X_{est} Y_{est} Z_{est}] coordinates are calculated by the following equations:

The range to the center of the transducer is estimated by averaging all of the calculated range values, if R $\gg$ x and R $\gg$ y, then:

$$R \approx \frac{R_1 + R_2 + R_3 + R_4}{4} \tag{28}$$

Path length differences are calculated for the left/right and up/down half-beams:

$$D_{rl} = R_{right} - R_{left} \tag{29}$$

$$D_{du} = R_{down} - R_{up} \tag{30}$$

Where R_{right}, R_{left}, R_{up} and R_{down} are the half beam estimates of the range to the target (see section 2.2.6). The left/right, up/down angles are calculated using the parallel ray approximation ($R \gg a$):

$$\theta_1 = \arcsin\left(\frac{D_{rl}}{a}\right) \tag{31}$$

$$\theta_2 = \arcsin\left(\frac{D_{du}}{a}\right) \tag{32}$$

Finally, the [X_{est} Y_{est} Z_{est}] locations are calculated from simple trigonometry:

$$X_{est} = R\sin\theta_1 \tag{33}$$

$$Y_{est} = R\sin\theta_2 \tag{34}$$

$$Z_{est} = \sqrt{R^2 - X_R^2 - Y_R^2} \tag{35}$$

where R_{left}, R_{right}, R_{down} and R_{up} are the half-beam ranges. D_{rl} is the right/left half-beam path length difference, D_{du} is the down/up half-beam path length difference, θ_1 and θ_2 are the left/right and up/down arrival angles and a is the separation between centers of the receivers.

The location of the fish using the measured phase is now determined. Path differences are calculated by subtracting the left/right and up/down half-beam phases and converting these phase differences to path lengths as described in section 2.1.3. A phase "lead" problem occurs when the phase on one half-beam wraps before the phase on the other half-beam (Figure 3). This phase "lead" is corrected by determining which phase half-beam phase leads and adding $\pm\pi$ when that phase no longer leads. The case when the initially leading phase no longer leads indicates that one of the phases wrapped and the other did not. Section 2.1.3 provides a discussion of the

algorithm to correct for phase lead.

The fish location is calculated for many different phase wraps by incrementing the path length difference d by $\pm\frac{\lambda}{2}$. The fish location is calculated in two-dimensions by using the geometry of the system to determine the angle of arrival of the pulse. Figure 14 shows a schematic of this geometry.

To find the location of the fish, calculate:

$$r_1 = \sqrt{(\frac{a}{2})^2 + R^2 - 2(\frac{a}{2})^2 R\cos(\frac{\pi}{2} - \theta)} \tag{36}$$

$$r_2 = \sqrt{(\frac{a}{2})^2 + R^2 - 2(\frac{a}{2})^2 R\cos(\frac{\pi}{2} + \theta)} \tag{37}$$

Where r_1 and r_2 are the ranges to the fish from receiver quadrants 1 and 2, a is the separation between receiver quadrant centers, R is the average range to the fish from the center of the transducer and θ is the angle of arrival of the pulse. If we numerically solve the following equation at values of $d = d \pm n\frac{\lambda}{2}$ for θ.

$$r_1 - r_2 - d = 0 \tag{38}$$

This operation is performed on both the left/right and up/down half-beams. If we constrain $\theta_1 < 90$ degrees and $\theta_2 < 90$ degrees, then $n = \frac{a}{\lambda}$ different choices for θ_1 and θ_2 are calculated from the phase of the returned signal. Using the location estimate obtained from the range values, the correct phase calculated location is selected from the grid of possible phase wrapped locations by choosing the location closest to the estimate obtained from the range calculation. The algorithm for calculating the fish location is shown in figure 15. The received pulses generated using the received pulse model described in figure 11 are used as input to the fish location extraction algorithm.

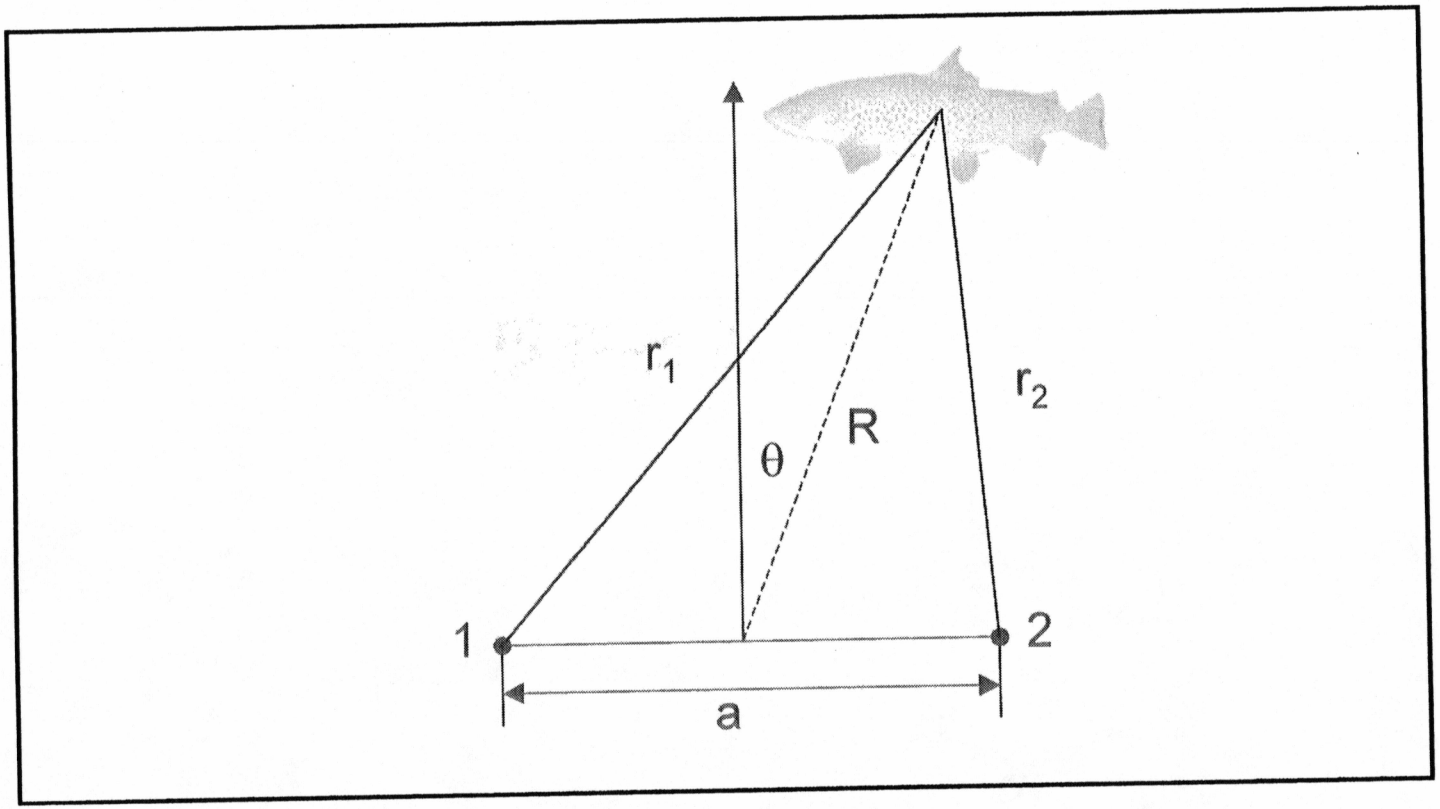

Figure 14. Fish location extraction geometry. Using simple geometry and trigonometry, we can determine the angle θ by numerical iteration. r_1 and r_2 are the ranges to the fish from locations 1 and 2. R is the range to the fish from the center of the transducer, and a is the separation between the transducer quadrant centers.

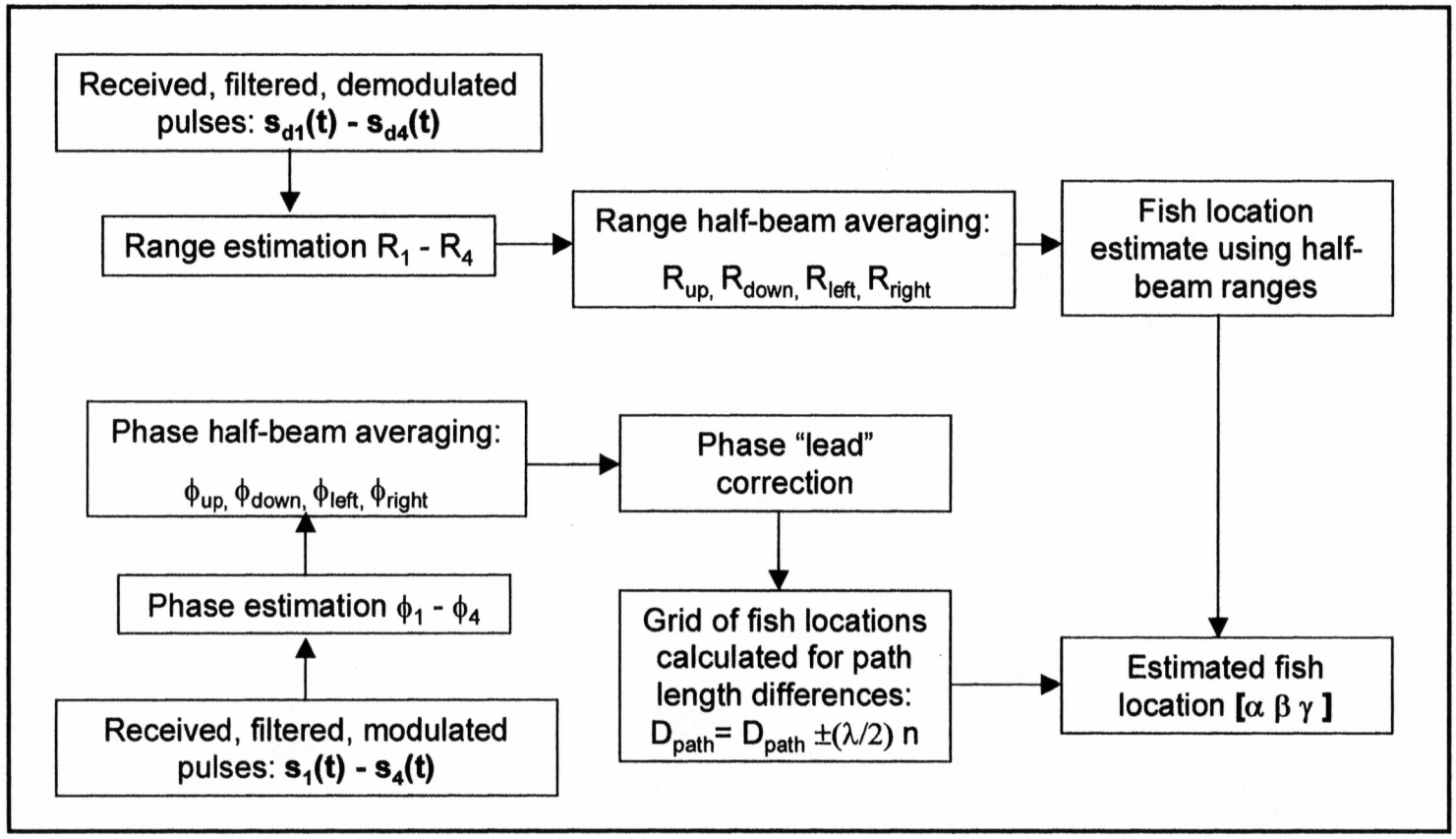

Figure 15. Fish location extraction flow diagram. This diagram shows the steps in locating the fish using the modulated and demodulated received pulses from each receiver. **Bold** type indicates input/output parameters.

The phases ϕ_1 - ϕ_4 are calculated by applying equations 21-23 to the received modulated signal at each quadrant. These phases are then averaged to obtain the half beam phases in equations 24-27. The phase of each quadrant is then corrected for phase lead. Once the phase of each quadrant is calculated, a grid of possible fish location is calculated using equation 38. The demodulated received signal at each quadrant is used to calculate an estimated range to the fish by estimating the time delay of the received pulse (see section 2.2.4). The range to each receiver quadrant is then used to calculate the half-beam ranges in the same manner as the half-beam phase (equations 24-27). The half beam ranges are then used to determine which phase wrap the fish lies in based on the calculated grid of possible fish locations.

3 Location Uncertainty

We discuss in this section the uncertainty in fish location due to signal to noise ratio, sampling frequency and pulse length. We shall find that the signal to noise ratio is the most important parameter in the split beam system. If the signal to noise ratio is less than 5 dB, then the fish location estimate will be poor.

3.1 Uncertainty due to Signal to Noise ratio

3.1.1 Stationary Fish Simulation

For the stationary fish simulations a fish is held fixed in a single location and 500 samples are taken of the fish location estimate with a fixed signal to noise ratio. Since the fish location uncertainty is dependent only on the received signal to noise ratio, the fish in these simulations is located in the center of the beam and signal to noise ratio is changed for convenience. In all of the stationary fish simulation figures, θ_1 is the x-axis and represents the left/right angle of arrival which is directly proportional to the x-coordinate position of the fish. θ_2 is the y-axis and represents the up/down angle of arrival which is directly proportional to the y-coordinate position of the fish.

The simulation is performed for signal to noise ratios of 15 dB, 5 dB, 3 dB and 0 dB. In all of the stationary fish simulations, the carrier frequency is 120 kHz and the sampling frequency is 1.2 MHz. The pulse width is 1 ms. The separation between the receiver elements is 10 cm and echo rise/fall time is 0.1 ms. The speed of sound in water is assumed to be 1500 m/s.

With signal to noise ratios of 15 dB and 5 dB the uncertainty in the location of the fish is primarily due to uncertainty in the phase measurement. For this reason identical results are obtained using both range estimation algorithms. Figure 16 shows

a scatter plot of 500 samples of the fish location x=0, y=0 and z = 15 meters with a signal to noise ratio of 15 dB. With a signal to noise ratio of 15 dB, the maximum variation in θ_1 is 2.39×10^{-3} degrees and the maximum variation in θ_2 is 2.32×10^{-3} degrees.

Figure 17 shows a scatter plot of fish locations with SNR = 5 dB. In the 5 dB case, errors in the phase measurement increase the maximum variation in θ_1 to 8.4×10^{-2} degrees and θ_2 to 7.3×10^{-2} degrees. When the signal to noise ratio is reduced to 3 dB, locating the fish accurately becomes more difficult. In this case, noise causes errors in both the phase and range estimates. If the estimated fish location using the range at each receiver is not accurate enough to select the correct phase wrap, phase wrap errors are introduced. Tables 1 and 2 provide statistics about the variation of θ_1 and θ_2 for all of the stationary fish simulations. The rows of tables 1 and 2 provide parameters that describe the uncertainty in the fish location estimate including mean, standard deviation and maximum variation for both θ_1 and θ_2. The columns of tables 1 and 2 give a description of which fish location algorithm was used to estimate the location of the fish. The dynamic noise estimate algorithm uses the dynamic noise estimate described in section 2.2.4. The matched filter estimate uses the matched filter algorithm described in section 2.2.4. The exact range algorithm calculates the location uncertainty with no error in the range estimate at each receiver quadrant. Although this is artificial it provides insight into the error in fish location uncertainty with no phase wrap ambiguity. Figure 18 shows the fish location uncertainty for a fish located at x=0, y=0 and z=15 meters with SNR = 3 dB. In this figure 5 discrete clouds can be seen. These clouds of uncertainty are due to the phase wrap condition.

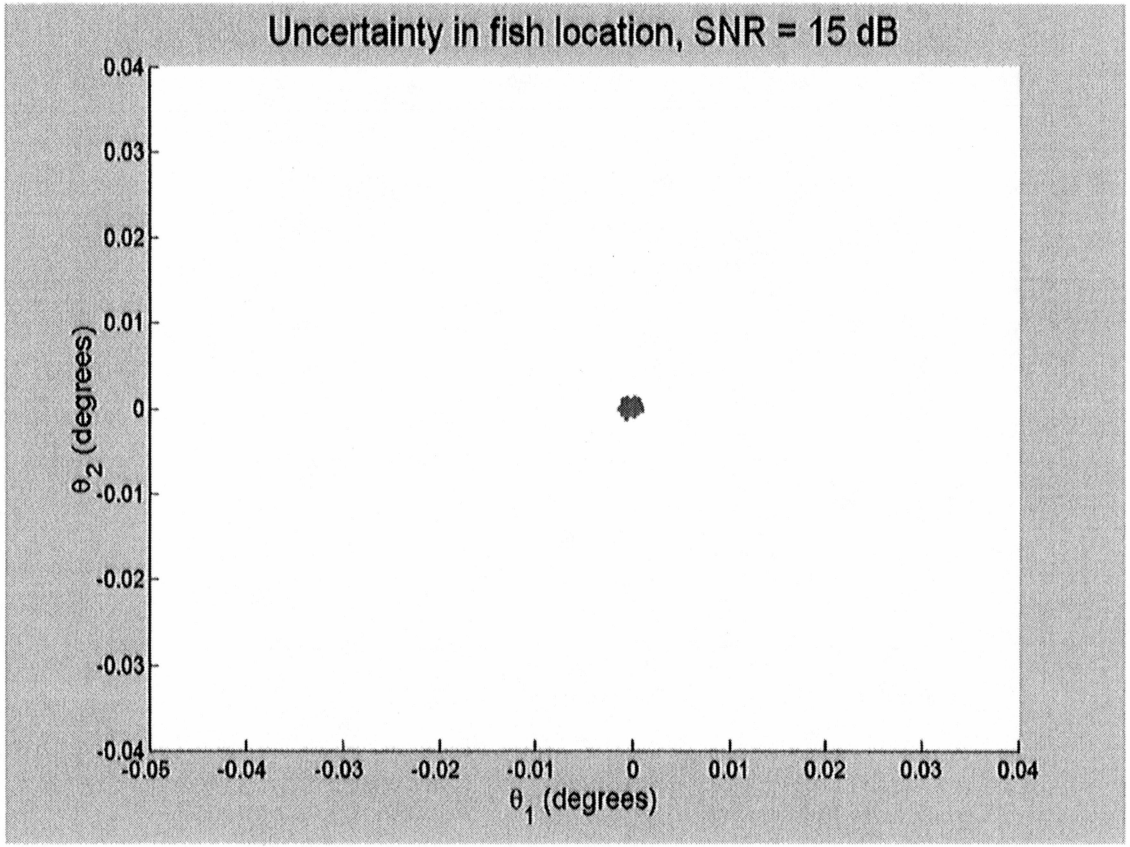

Figure 16. Uncertainty in fish location, SNR = 15 dB. Fish located at [0 0 15] meters. No phase wrap occurs so the uncertainty is primarily due to phase measurement error. θ_1 is the left/right angle and θ_2 is the up/down angle.

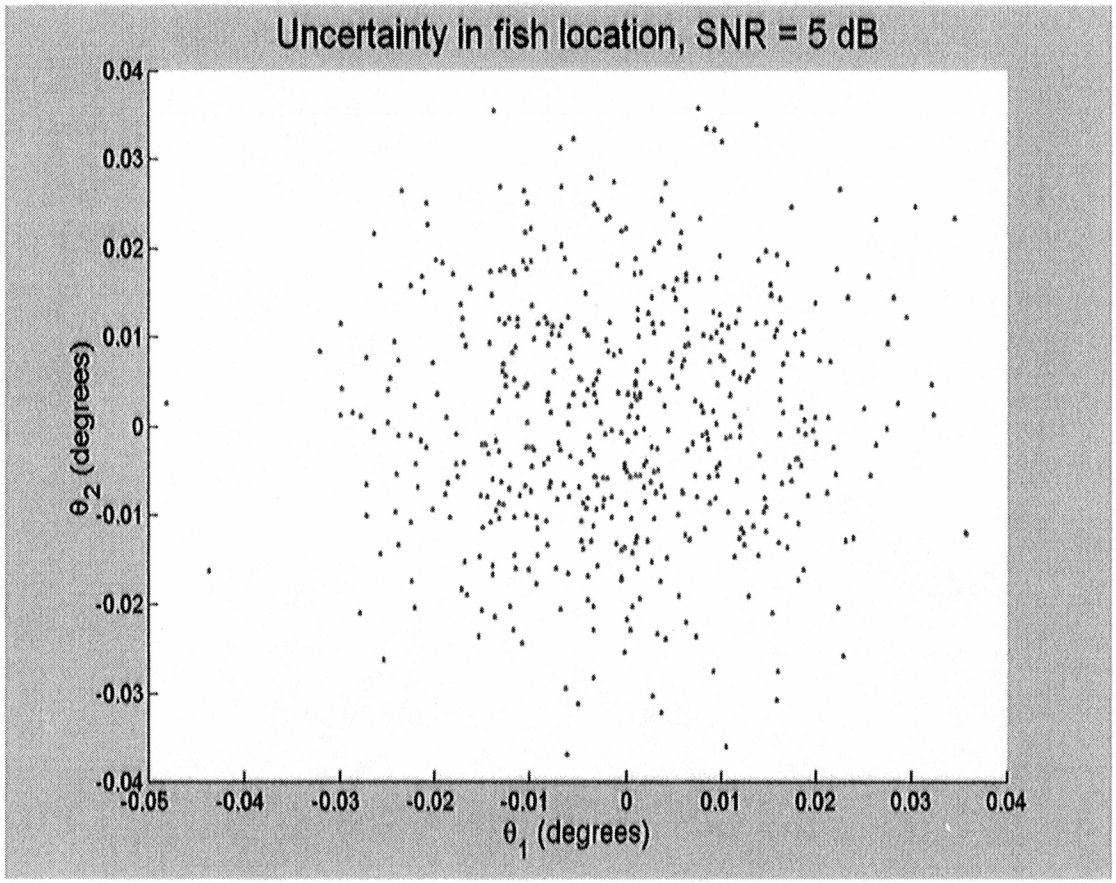

Figure 17. Uncertainty in fish location, SNR = 5 dB. Fish located at [0 0 15] meters. Uncertainty in fish location is primarily due to phase uncertainty. θ_1 is the left/right angle and θ_2 is the up/down angle.

	SNR = 15 dB	SNR = 5 dB	SNR = 3 dB		
Parameter	Dynamic noise estimate	Dynamic noise estimate	Dynamic noise estimate	Matched filter estimate	exact range
mean θ_1 (deg)	-0.000017	-0.000424	-0.013968769	0.071838749	-0.001490
mean θ_2 (deg)	-0.000004	0.000688	-0.020759081	0.021132602	0.000474
std θ_1 (deg)	0.000381	0.013735	0.554106776	1.699720079	0.026699
std θ_2 (deg)	0.000385	0.013544	0.53253184	1.708404347	0.027515
$\Delta\theta_1$ (deg)	0.002390	0.083873	7.177416542	18.29901979	0.166051
$\Delta\theta_2$ (deg)	0.002323	0.072658	7.212615156	18.18721558	0.160910
mean x (cm)	-0.000446	-0.011097	-0.365702	1.880735	-0.039007
mean y (cm)	-0.000107	0.018004	-0.543471	0.553250	0.012407
std x (cm)	0.009963	0.359586	14.506934	44.511626	0.698974
std y (cm)	0.010068	0.354585	13.942052	44.739181	0.720343
Δx (cm)	0.062581	2.195793	188.893428	496.049102	4.347212
Δy (cm)	0.060814	1.902181	189.829612	492.804058	4.212618

Table 1. Stationary fish simulation statistics. The fish location uncertainty is modeled for SNR = 15 dB, SNR = 5 dB, SNR = 3 dB cases. In the 15 dB and 5 dB cases, the uncertainty is primarily due to phase measurement error. In the 3 dB case, error occurs in both the phase wrap determination and phase measurement. Results are presented for both range estimation algorithms, and when the phase wrap region is known exactly in the 3 dB case.

	SNR = 0 dB		
Parameter	Dynamic noise estimate	Matched filter estimate	exact range
mean θ_1 (deg)	0.103491054	0.272770797	0.001441
mean θ_2 (deg)	-0.016413891	-0.071659157	0.001134
std θ_1 (deg)	3.715379207	6.091700745	0.069263
std θ_2 (deg)	3.827508129	6.177263969	0.074315
$\Delta\theta_1$ (deg)	25.83922885	29.58196932	0.423831
$\Delta\theta_2$ (deg)	25.90363944	32.89621066	0.438467
mean x (cm)	2.709392	7.141177	0.037735
mean y (cm)	-0.429715	-1.876033	0.029675
std x (cm)	97.404966	160.084004	1.813314
std y (cm)	100.353251	162.349920	1.945570
Δx (cm)	726.395766	851.494332	11.096085
Δy (cm)	728.478615	970.252801	11.479259

Table 2. Stationary fish simulation statistics continued. The fish location uncertainty is modeled for the SNR = 0 dB case. In the 0 dB case, error occurs in both the phase wrap determination and phase measurement. Results are presented for both range estimation algorithms, and also for the case when the phase wrap region is known exactly.

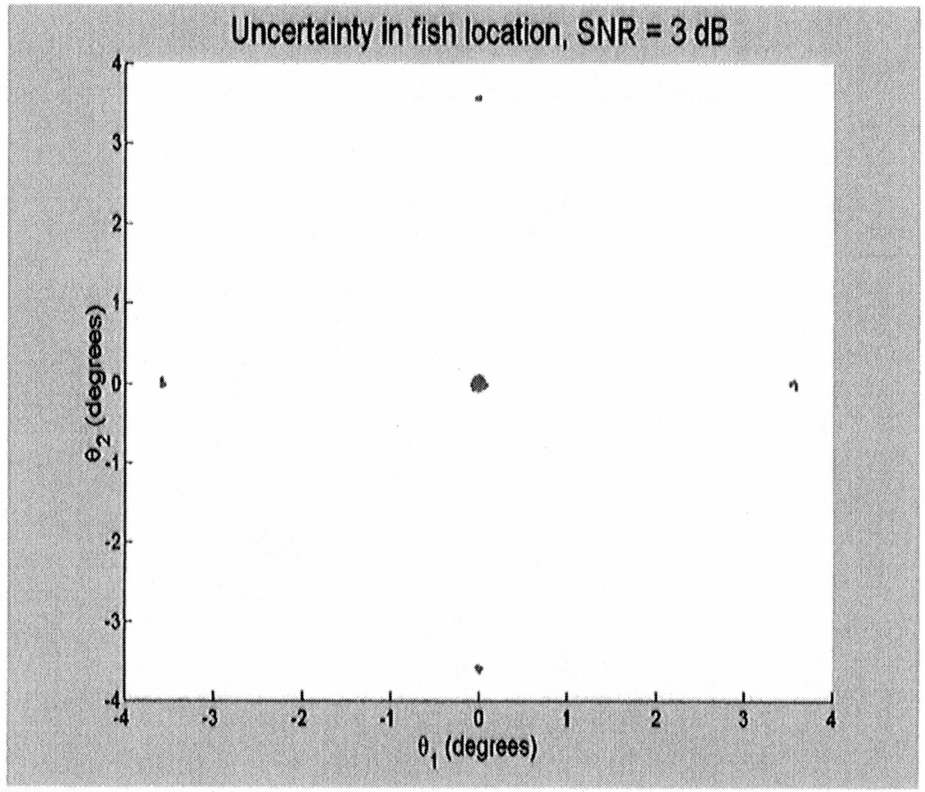

Figure 18. Uncertainty using dynamic noise estimate range algorithm, SNR = 3 dB. Fish located at [0 0 15] meters. Inaccurate range estimates cause phase wrap ambiguities. θ_1 is the left/right angle and θ_2 is the up/down angle. Discrete clouds are present when the fish location algorithm selects the wrong phase wrap condition. (see text)

The grid of fish locations is calculated based on the received phase at each receiver quadrant and these possible fish locations are compared to the fish location estimate using the calculated time delay. If the location estimate using the calculated time delay is selects the wrong grid location, then the fish location estimate will appear in the wrong location. It is clear that the clouds in the center and at each of the cardinal locations nearest the center exhibit this grid based behavior. This simulation was performed using both the dynamic noise estimate and matched filter algorithms described in Section 2.2.4. The results presented in figure 18 were obtained using the dynamic noise estimate algorithm. The maximum variation in θ_1 and θ_2 is 7.2 degrees.

Reducing the signal to noise ratio to 0 dB causes larger errors in the fish location estimate. The range estimation algorithms developed in this model work poorly when the signal to noise ratio is less than 5 dB. For this reason, phase wrap errors are common. Figure 19 shows the scatter plot of fish location uncertainty when SNR = 0 dB. In the 0 dB case, the maximum variation is 25.9 degrees in both the θ_1 and θ_2 directions. This large variation is primarily due to the large uncertainty in the estimate of pulse arrival time. The discrete locations in the low SNR figures are due to errors in the range and phase estimates which cause the wrong phase wrap to be chosen. These errors are explained by the way the algorithm selects the correct fish location. The algorithm generates a grid of possible fish locations from the measured phase and compares that grid with the location estimate obtained from range differencing (Section 2.2.7). The location estimate calculated from the received phase that is closest to the range difference estimate is chosen as the correct value. This method works well when the range difference estimate errors are less than a wavelength.

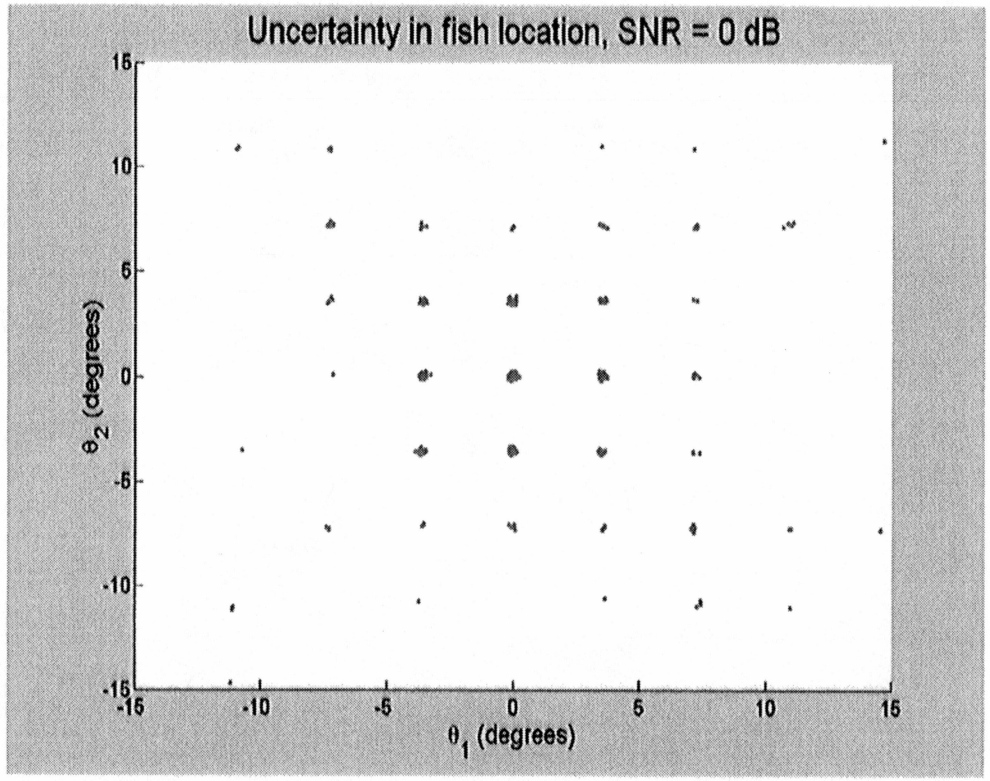

Figure 19. Uncertainty using dynamic noise estimate range algorithm, SNR = 0 dB. Fish located at [0 0 15] meters. Inaccurate range estimates cause phase wrap ambiguities. θ_1 is the left/right angle and θ_2 is the up/down angle. Discrete clouds are present when the fish location algorithm selects the wrong phase wrap condition. (see text)

The uncertainty due to choosing the wrong phase wrap is significantly larger than the uncertainty due phase error alone. Tables 1 and 2 provide statistics for additional data not present in the figures. This includes sample mean, standard deviation, and overall variation for 4 SNR levels using different range measurement algorithms. If the exact range values are used to remove the phase wrap ambiguity, then the uncertainty due to phase measurement can be estimated. The "exact" range measurement algorithm is used to show the variation due to phase uncertainty alone. As can be seen from Tables 1 and 2, if the phase wrap ambiguity is known, the error in fish location is relatively small, but if the phase wrap errors occur, the uncertainty becomes large. Thus, removing the phase wrap is the hardest part of obtaining an accurate fish location estimate.

3.1.2 Fish Track Simulation

Two fish tracks were created to demonstrate the variation of the estimated fish location as a fish moves through the beam of the transducer. Two different simulations are performed for each fish track to provide a better visualization of the uncertainty.

Fish track A moves a simulated fish from x = -1.5 meters to x = 1.5 meters. In this track y = 0 meters and z = 30 meters. These x values were chosen to keep the fish in the main lobe of the beam and thus minimize the chance of phase wrap ambiguities. If we assume that the sidelobe level of the transducer is sufficiently low, then all of the returns will be from the main lobe of the transducer. Since the transducer is rectangular, no phase wrap occurs in the main lobe of the transducer beam as shown in Figure 2. Figure 20 shows the setup for simulation A, including the orientation of the fish. The simulated tracks in Figure 21 show that the location uncertainty increases as the fish moves further out of the center of the beam.

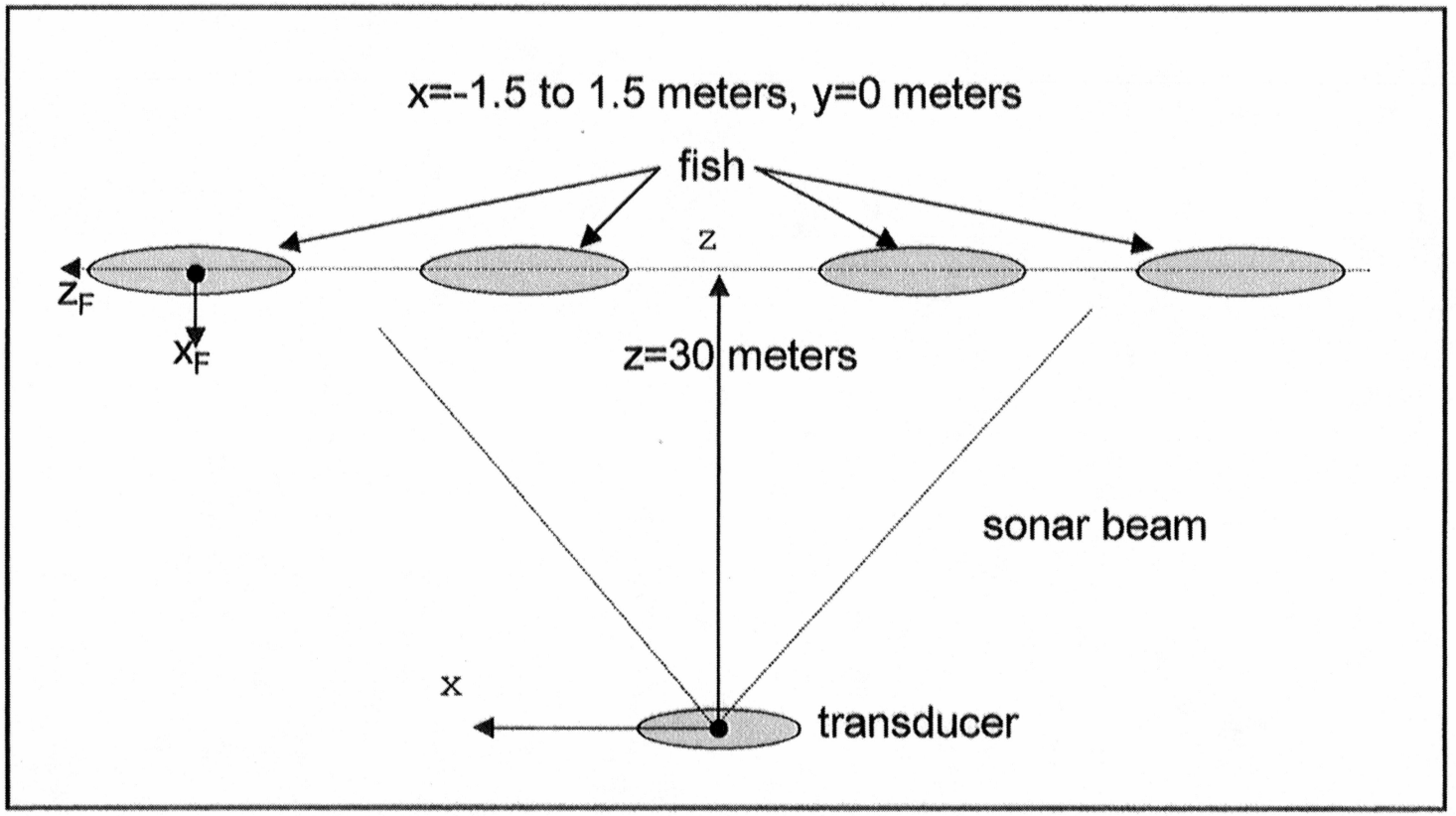

Figure 20. Simulation setup for fish track A. Fish is moving from x = -1.5 meters to x = 1.5 meters with y = 0 meters and z = 30 meters. This puts the fish in the main lobe of the transducer beam. y_F is out of the page.

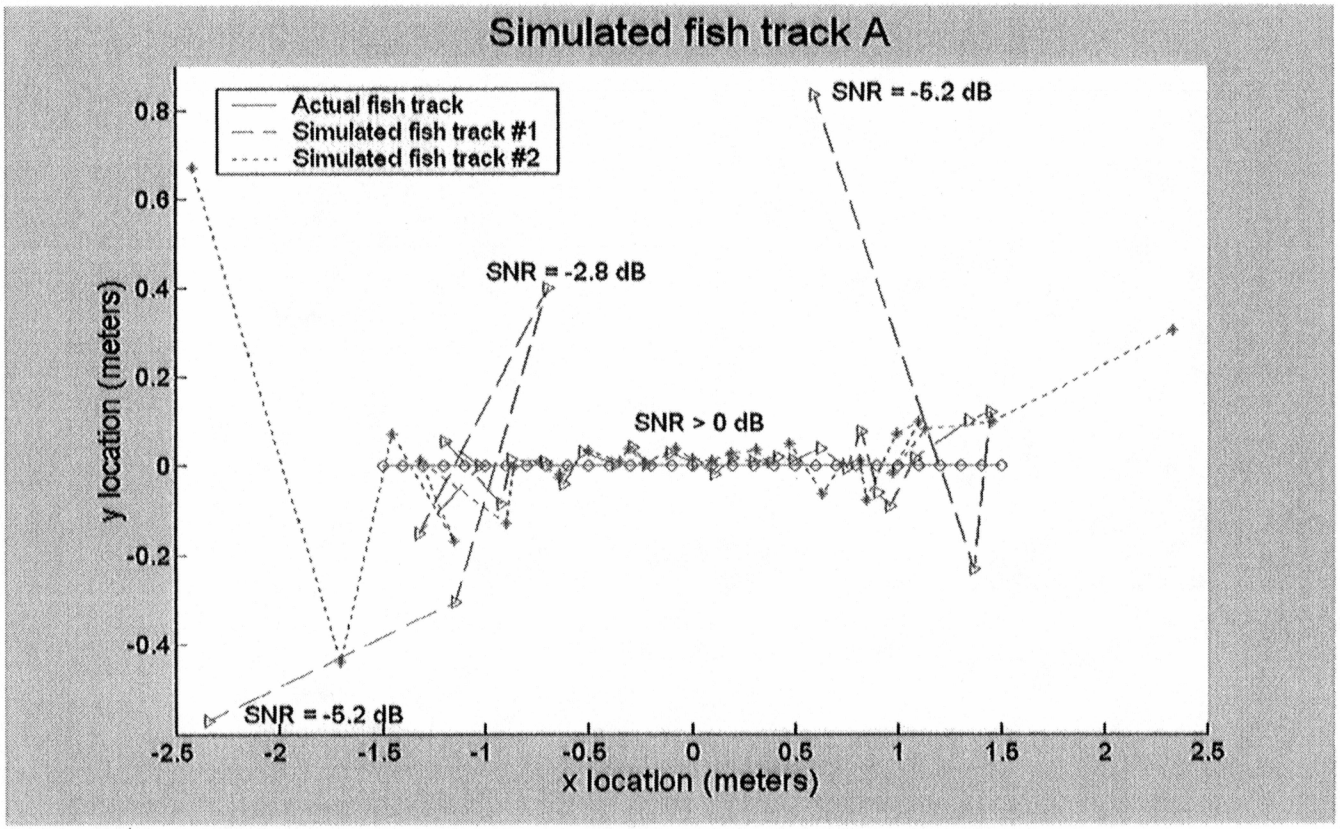

Figure 21. Simulated fish track A. Fish is moving from x = -1.5 meters to x = 1.5 meters with y = 0 meters and z = 30 meters. This puts the fish in the main lobe of the transducer beam and removes any phase wrap ambiguity. A few SNR values are included on the figure for reference. Two simulated tracks are provided.

Figure 22 shows the signal to noise ratio as a function of x location. The signal to noise ratio of the received signal is calculated using the sonar equation described in Section 2.1.5. The level of SNR_{ref} is set to 80 dB for both of the simulations performed using fish track A to provide an appropriate range of received signal to noise ratio levels. Thus,

$$\mathrm{SNR}_{rcvd} = \mathrm{SNR}_{ref} + TL + BF + TS \tag{39}$$

Where the SNR_{rcvd} is the signal to noise ratio after all of the losses have been removed. TL (transmission loss), BF (beam factor), and TS (target strength) all change as the fish moves through the beam of the transducer. Since the primary loss in simulation A is due to the changing beam pattern, the signal to noise ratio plot in Figure 21 closely resembles the beam pattern of the transducer. The signal to noise ratio also decreases as the fish moves out of the beam because of smaller effects due to range and changing target strength. Approximately 8 dB of SNR variation results in a location uncertainty of about 0.8 meters as the fish moves across the beam. Fish track B shown in figure 23 simulates a fish moving away from the transducer from z = 5 meters to z = 30 meters. The value of SNR_{ref} = 80 dB is selected to provide an appropriate range of signal to noise ratios in fish track B. The orientation of the simulated fish is different from the orientation in fish track A. The fish body is pointed away from the transducer, providing a lower target strength. Since, the signal to noise ratio change is primarily due to the spreading loss as the fish moves further away from the transducer, the pressure signal to noise ratio decreases as ($\sim \frac{1}{R^2}$) with increasing z location. In fish track B, the signal to noise ratio has a range of approximately 30 dB.

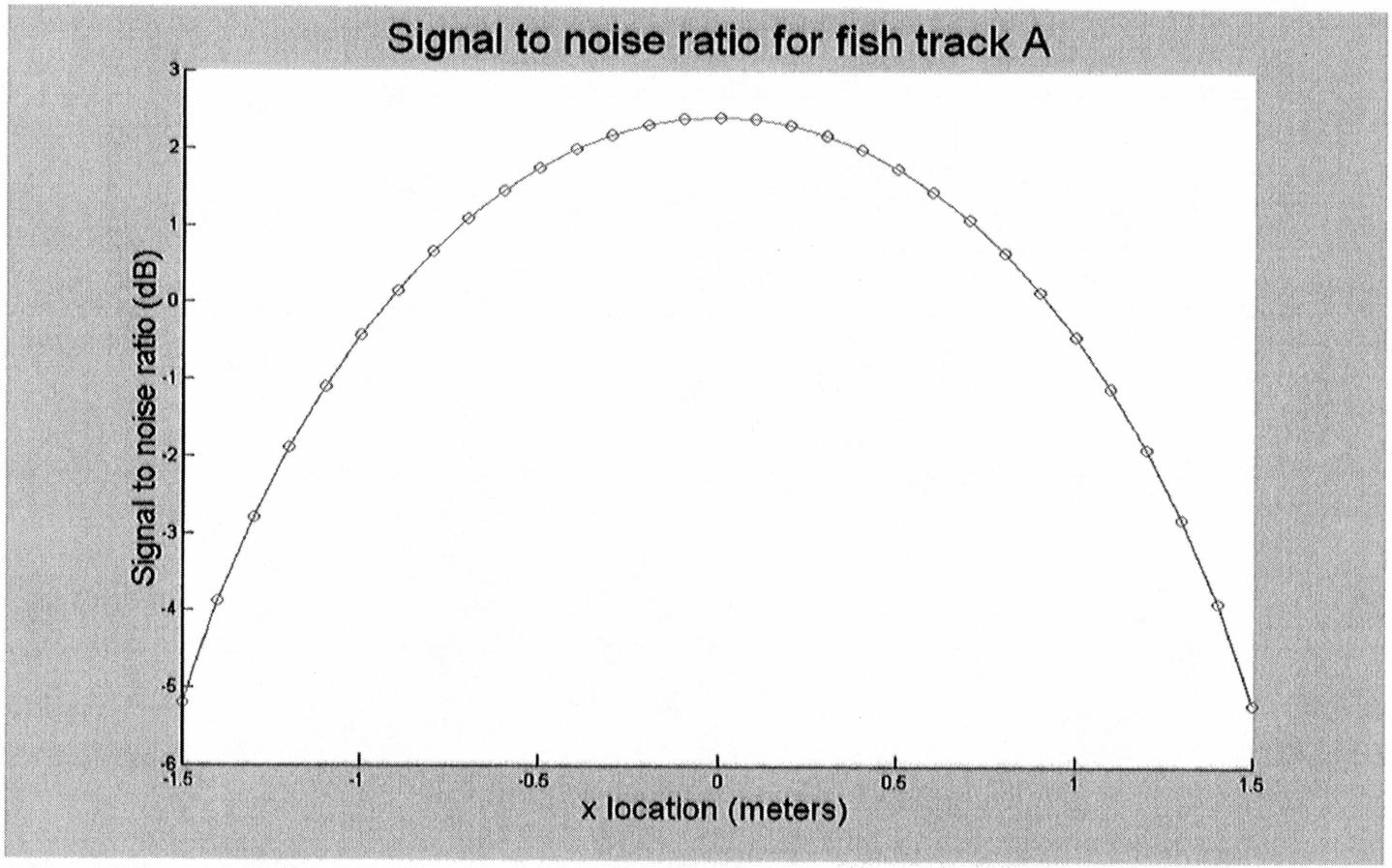

Figure 22. Signal to Noise ratio for fish track A. The signal shows a variation of about 8 dB, this results in about 100 - 150 cm of error in both the x and y location estimates.

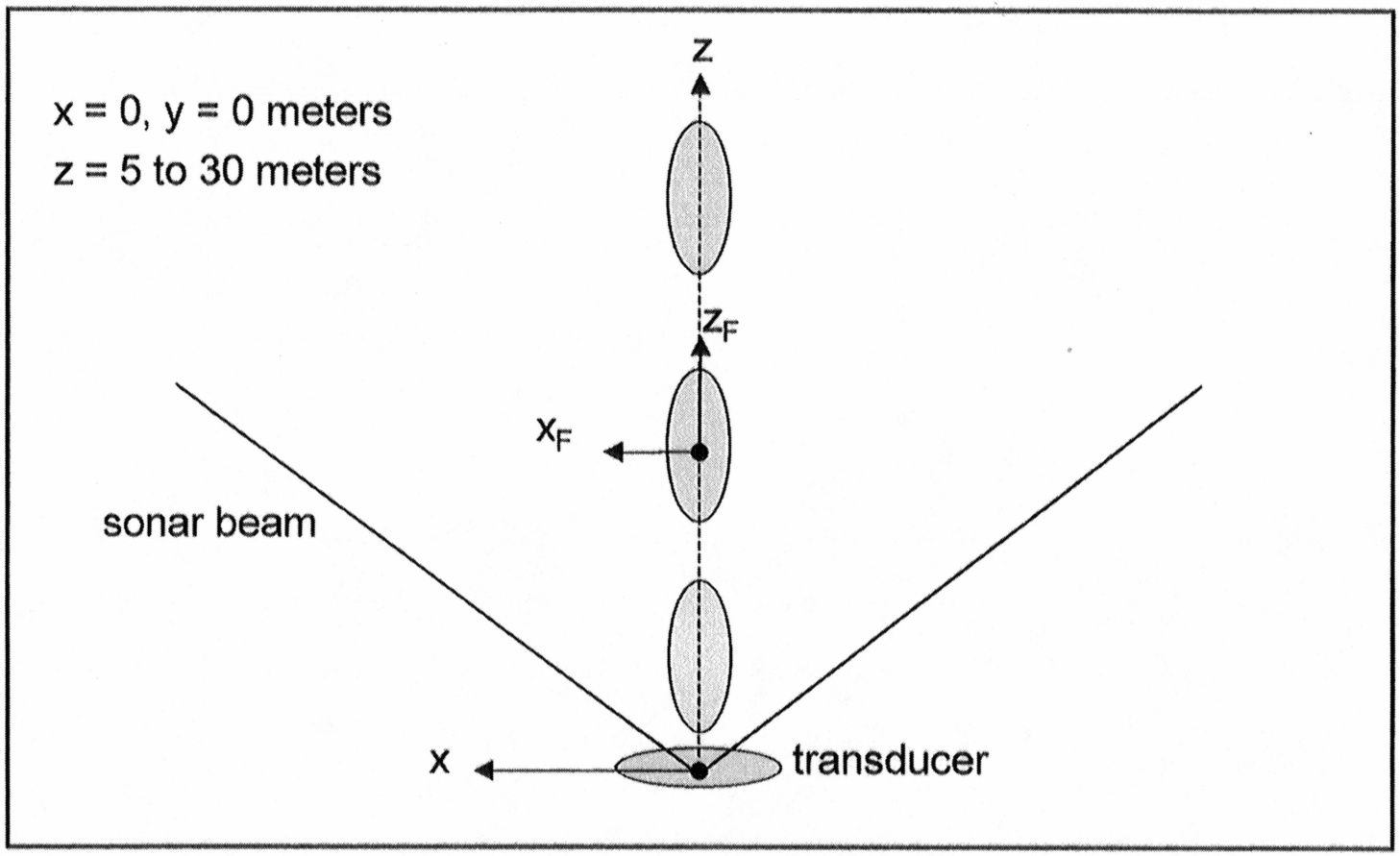

Figure 23. Simulation setup for fish track B. Fish is moving from z = 5 meters to z = 30 meters with y = 0 meters and x = 0 meters. Y_F is out of the page.

In figures 24 and 25 when the signal to noise ratio drops below 5 dB the uncertainty is approximately 1 meter in both the x and y directions. Figure 26 shows the signal to noise ratio vs. z location for fish track B. A comparison of the signal to noise ratio plots from fish tracks A and B shows that similar results are obtained when the signal to noise ratio drops below 5 dB. This agrees with the stationary fish simulation.

3.2 Uncertainty due to sampling frequency

The sampling frequency used in the split beam system has a significant effect on the overall accuracy of the location estimate. If the sampling frequency is not large enough, errors will occur in the measured phase and range. The sampling frequency required for reliable operation is approximately $5f_c$, where f_c is the carrier frequency of the pulse. Filtering the modulated pulse does not appear to decrease the sampling frequency requirement. More sophisticated filtering algorithms may help to decrease the required sampling frequency. In general, as the sampling frequency is decreased, the uncertainty in the measured phase and range increases. Table 3 shows the maximum variation and standard deviation of 500 samples of θ_1 and θ_2 at 3 different sampling frequencies and signal to noise ratios of 15 dB and 3 dB. In the simulation the fish is assumed to be in the main lobe of the transducer and thus no phase wrap occurs. The fish is located at [0 0 15] meters, the carrier frequency used is 120 kHz, the pulse width is 1 ms and the rise and fall times t_r are 1 ms. The separation between receiver centers is 10 cm. For the SNR = 15 dB case with a sampling frequency 1.2 MHz ($10f_c$), the maximum variation in θ_1 and θ_2 is approximately 2.5×10^{-3} degrees. This is the same result that was obtained in the stationary fish simulation.

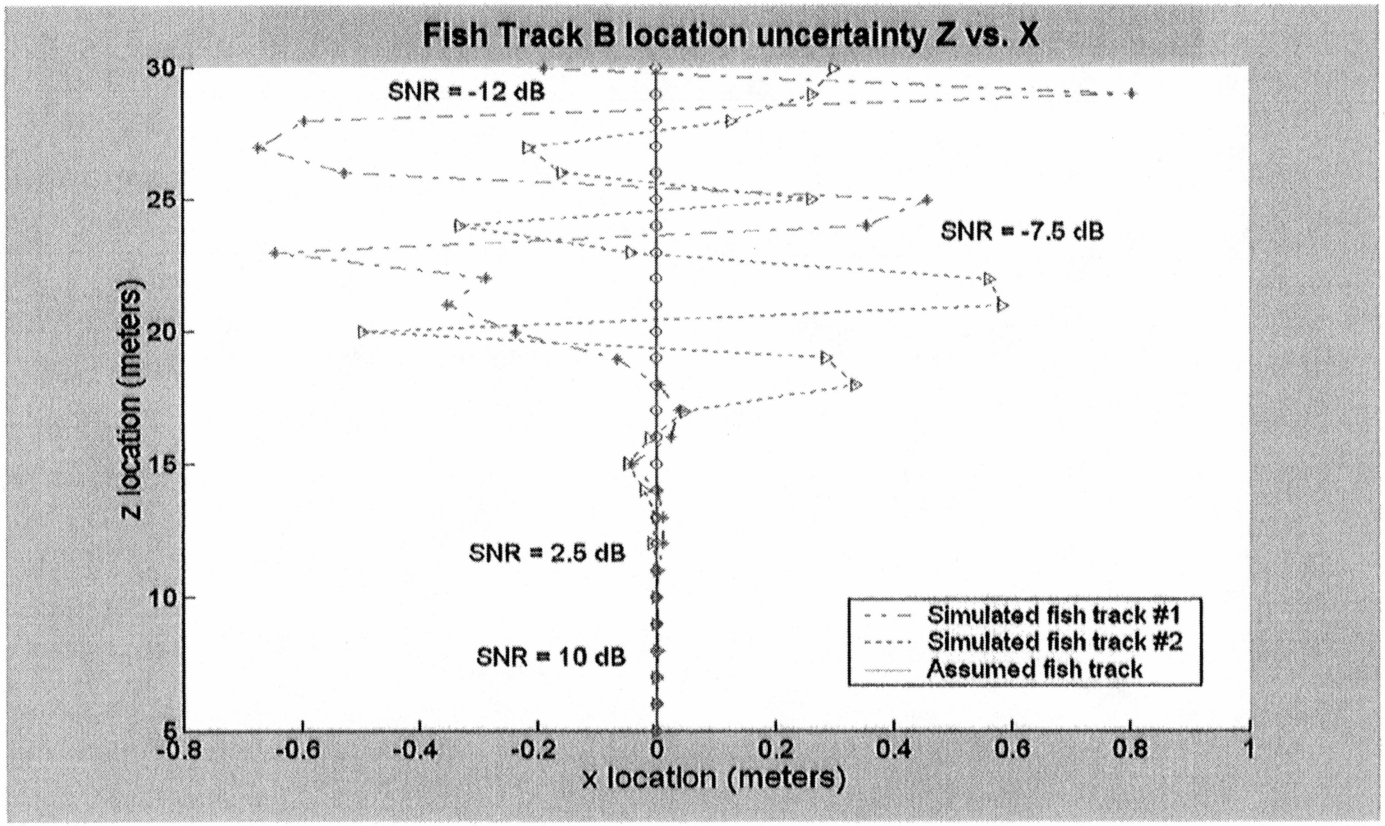

Figure 24. Simulated fish track B, Z vs. X. The fish is located at x=0, y=0 meters and moves from z=5 meters to z=30 meters. Two uncertain tracks are provided to give a better feel for the variation in the location estimate.

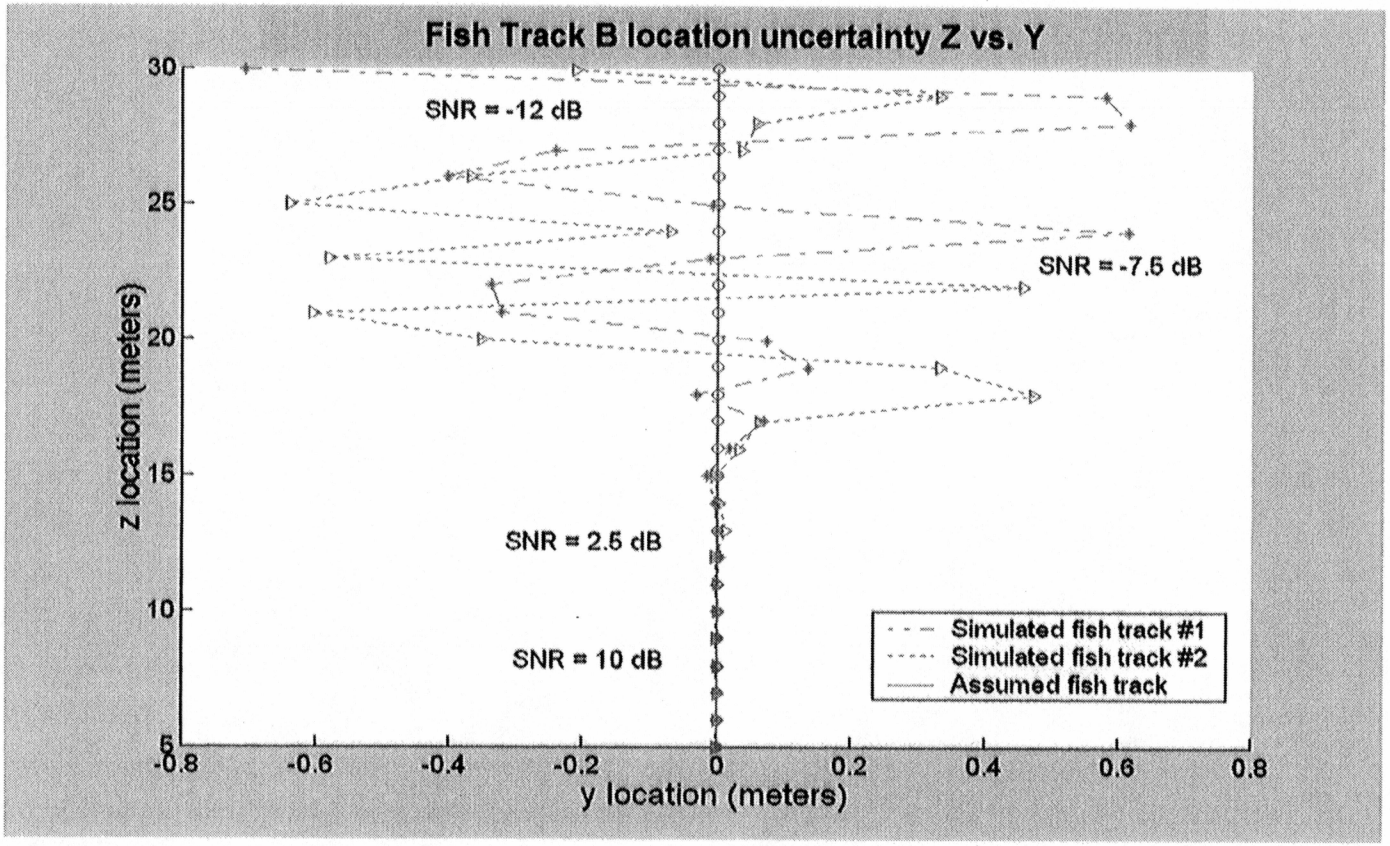

Figure 25. Simulated fish track B, Z vs. Y. The fish is located at x=0, y=0 meters and moves from z=5 meters to z=30 meters. Two uncertain tracks are provided to give a better feel for the variation in the location estimate.

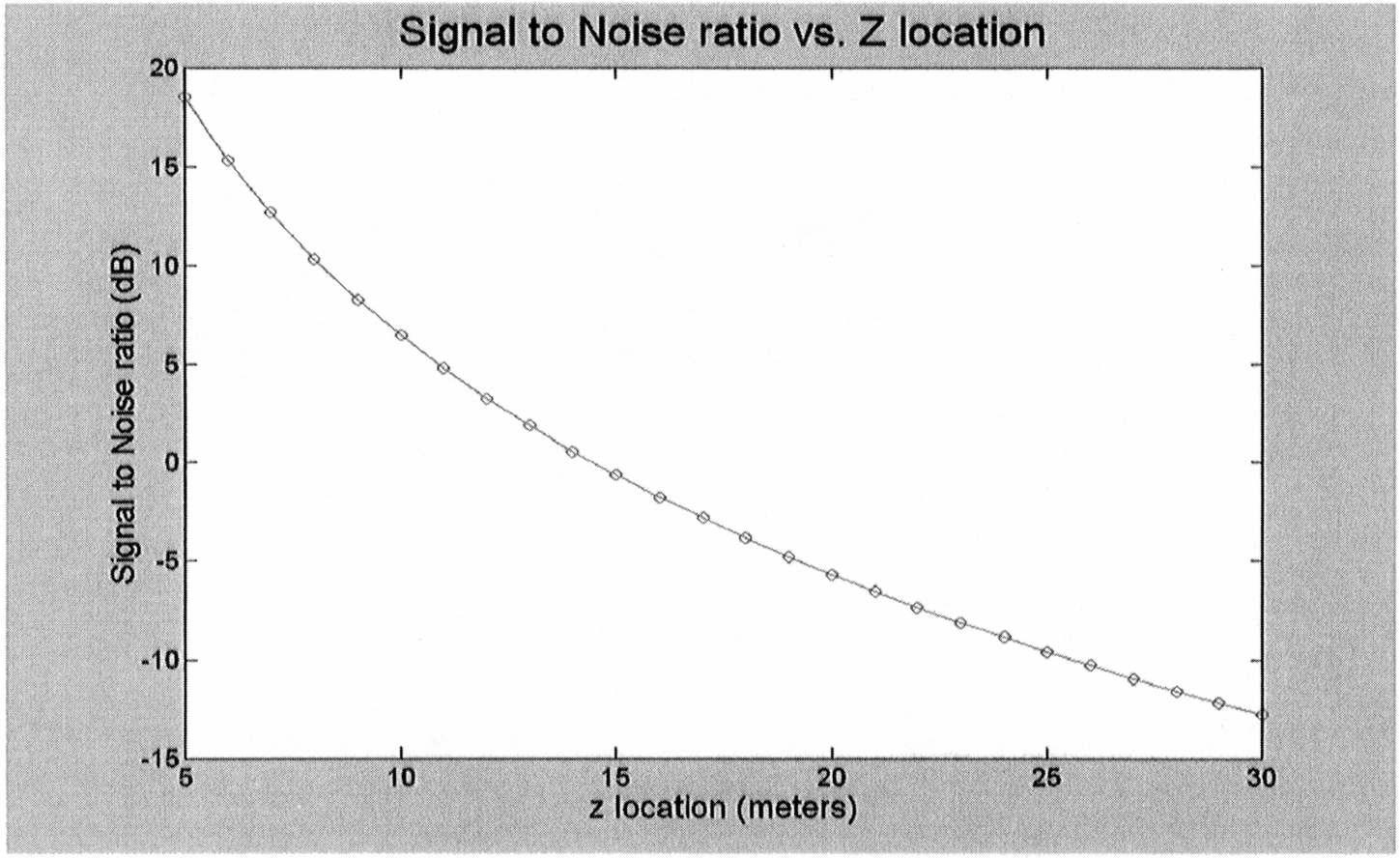

Figure 26. Signal to noise ratio vs. Z location for fish track B. The signal to noise ratio is primarily dependant on the spreading loss.

Varying Sampling Frequency: SNR = 15 dB					
Sampling Freq (kHz)	Mean θ_1 (degrees)	Mean θ_2 (degrees)	Std θ_1 (degrees)	Std θ_2 (degrees)	$\Delta\theta_1$ (degrees)
300	0.000032	0.000061	0.000873	0.000845	0.005597
600	-0.000001	-0.000001	0.000614	0.000593	0.003665
1200	0.000018	-0.000022	0.000434	0.000422	0.002577
Sampling Freq (kHz)	Mean x (cm) @ z = 15 m	Mean y (cm) @ z = 15 m	Std x (cm) @ z = 15 m	Std y (cm) @ z = 15 m	Δx (cm) @ z = 15 m
300	0.000844	0.001605	0.022854	0.022130	0.146526
600	-0.000029	-0.000032	0.016076	0.015536	0.095937
1200	0.000475	-0.000585	0.011361	0.011047	0.067470
Varying Sampling Frequency: SNR = 3 dB					
Sampling Freq (kHz)	Mean θ_1 (degrees)	Mean θ_2 (degrees)	Std θ_1 (degrees)	Std θ_2 (degrees)	$\Delta\theta_1$ (degrees)
300	0.000978	0.001013	0.054900	0.057663	0.343743
600	0.001843	-0.001154	0.039049	0.039913	0.246456
1200	-0.000011	0.000003	0.000446	0.000440	0.002638
Sampling Freq (kHz)	Mean x (cm) @ z = 15 m	Mean y (cm) @ z = 15 m	Std x (cm) @ z = 15 m	Std y (cm) @ z = 15 m	Δx (cm) @ z = 15 m
300	0.025611	0.026528	1.437284	1.509610	8.999267
600	0.048249	-0.030213	1.022312	1.044915	6.452242
1200	-0.000280	0.000066	0.011674	0.011530	0.069059

Table 3. Uncertainty due to sampling frequency statistics, SNR = 15 dB, 3 dB. This table shows the mean, standard deviation and maximum variation of θ_1 and θ_2 for sampling frequencies of 300, 600, and 1200 kHz. The signal to noise ratio is fixed at 15 dB and 3 dB. Pulse width is 1 ms, pulse rise time is 1 ms, and the modulation frequency is 120 kHz. The fish is located at [0 0 15] meters.

Reducing the sampling frequency to 600 ($5f_c$) kHz degrades the fish location accuracy. The maximum variation is now approximately 3.5×10^{-3} degrees. Decreasing the sampling frequency to 300 kHz ($2.5f_c$) causes the estimation error to increase further. The maximum variation is approximately 5.5×10^{-3} degrees. Reducing the sampling frequency produces fish location results similar to reducing the signal to noise ratio.

3.3 Uncertainty due to pulse duration

The transmitted pulse duration has a significant effect on the accuracy of the fish location estimate. As the pulse duration is reduced, the uncertainty in the location of the fish increases. The inherent averaging in the in-phase/quadrature method of phase measurement leads to better results with longer pulses. Simulation results show that choosing a pulse duration that is greater than 100 cycles (1 ms @ 120 kHz) is adequate to provide good results at any signal to noise ratio.

Table 4 shows the maximum variation and standard deviation of 500 samples of θ_1 and θ_2 for 4 different pulse durations and signal to noise ratios of 15 dB and 3 dB. The fish is located at [0 0 15] meters. The carrier frequency is 120 kHz and the sampling frequency is 1.2 MHz.

Although error increases in the phase measurement, pulse length does not effect the range measurement. The range is measured using the rising edge of the received pulse, so increasing the length of the pulse has no effect on the range uncertainty. Since the in-phase/quadrature method of phase measurement averages over the pulse duration to measure the in-phase and quadrature components of the signal, making the pulse longer gives better phase measurement results. This suggests that the choice of sampling frequency is more critical than the choice of pulse duration.

SNR = 15 dB

Pulse Width (ms)	Std θ_1 (degrees)	Std θ_2 (degrees)	$\Delta\theta_1$ (degrees)	$\Delta\theta_2$ (degrees)
0.10	0.003834	0.003719	0.024409	0.021215
1.00	0.000425	0.000432	0.002632	0.002801
5.00	0.000101	0.000106	0.000593	0.000760
10.00	0.000062	0.000058	0.000391	0.000367
Pulse Width (ms)	**Std x (cm) @ z = 15 m**	**Std y (cm) @ z = 15 m**	**Δx (cm) @ z = 15 m**	**Δy (cm) @ z = 15 m**
0.10	0.100366	0.097373	0.639022	0.555403
1.00	0.011136	0.011308	0.068914	0.073331
5.00	0.002640	0.002775	0.015513	0.019890
10.00	0.001614	0.001515	0.010241	0.009611

SNR = 3 dB

Pulse Width (ms)	Std θ_1 (degrees)	Std θ_2 (degrees)	$\Delta\theta_1$ (degrees)	$\Delta\theta_2$ (degrees)
0.10	0.331100	0.324946	2.467030	3.012616
1.00	0.027224	0.027097	0.167637	0.161965
5.00	0.006366	0.005846	0.042822	0.034329
10.00	0.003647	0.003633	0.021916	0.021283
Pulse Width (ms)	**Std x (cm) @ z = 15 m**	**Std y (cm) @ z = 15 m**	**Δx (cm) @ z = 15 m**	**Δy (cm) @ z = 15 m**
0.10	8.668277	8.507152	64.626648	78.942872
1.00	0.712714	0.709388	4.388748	4.240250
5.00	0.166661	0.153055	1.121073	0.898739
10.00	0.095486	0.095124	0.573771	0.557175

Table 4. Uncertainty due to pulse duration statistics. This table shows the standard deviation and maximum variation for four different pulse durations and two signal to noise ratios. The fish is located at [0 0 15] meters. The sampling frequency is 1.2 MHz, the modulation frequency is 120 kHz and the rise/fall time is 0.1 ms. As the pulse width is reduced, the errors in the angles of arrival θ_1 and θ_2 increase.

3.4 Comparison with Chandalar River data

3.4.1 Simulation set-up

The real data used in this thesis was collected by Mr. Dave Daum of the U.S. Fish and Wildlife Service. The data was collected in 1995 during a five year hydroacoustic study on the Chandalar River, Alaska. A split beam sonar system was setup at a river site to count adult fall chum salmon. Gill netting and catch statistics from previous years confirmed that chum salmon made up 99% of the fish population. The average fish size from the catch group was 59 cm. U.S. Fish and Wildlife employees conducting the experiment attached helium balloons to 42 fish using string and *in situ* target strength measurements were made. The split beam sonar system used consisted of two Hydroacoustic Technology, Inc. (HTI) split beam systems operating at 200 kHz using elliptical transducers with beam widths of 4.6 by 10.8 degrees and 2.8 by 11.3 degrees. The transmitted pulse width was 0.2 ms [Daum and Osborne 1996]. The data contains measured [x y z] coordinates for sonar tracked fish as well as beam factor and target strength estimates.

3.4.2 Simulation results

In this simulation, a single noisy recorded track is simulated using the measured [x y z] coordinates, beam factor, and target strength provided by the data. The simulation parameters are as follows. The reference signal to noise ratio is set to $\mathrm{SNR}_{ref} = 95$ dB to provide a realistic range of signal to noise ratio values as the fish passes through the transducer beam. $T_P = 0.2$ ms, $T_R = 10\mu$s, $f_c = 200$ kHz, $c = 1500$ m/s, and $a = 10$ cm in all of the simulations. Where SNR_{ref} is the source SNR level, T_P is the pulse duration, T_R is the pulse rise/fall time, f_c is the pulse carrier frequency, c is the speed

of sound in water, and a is the center-to-center receiver separation. The rectangular transducer array described earlier in the thesis is used in this simulation. Since the beam factor values used from the measured data are used in this simulation, the only errors introduced by using this rectangular arrangement will be from receiver separation differences. The fish is assumed to be located in the main lobe of the transducer and no phase wrap errors are allowed in the simulated data.

Figures 27, 28 and 29 show plots of x location vs. y location for the collected Chandalar and simulated Chandalar River data. Figure 30 shows a plot of the signal to noise ratio vs. time for the simulated received echoes. In the higher SNR region, the fish location is well defined and difference between the simulated and collected data is present. As the fish moves through the beam of the transducer the SNR decreases and the fish location becomes more uncertain. The simulated data shows that the fish could have been located in the simulated locations with the same probability as being located in the measured locations at the given SNR values.

If the reference signal to noise ratio SNR_{ref} was chosen to be something other than 95 dB, it would result is a linear shift in the y axis of figure 30. The value that is chosen for SNR_{ref} simply sets the reference level around which the signal to noise ratio will vary.

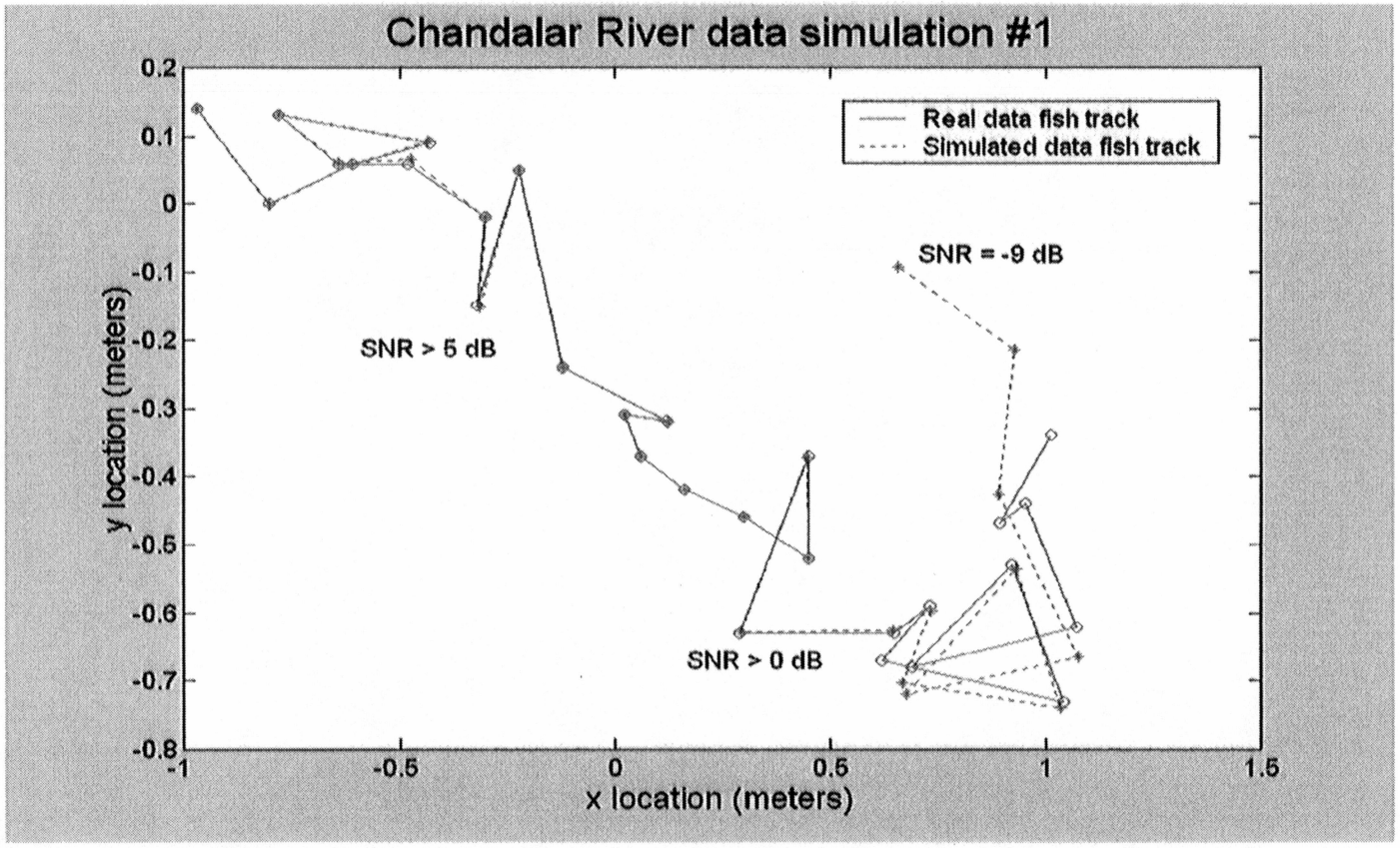

Figure 27. Chandalar River data simulation #1. This figure shows data collected from Chandalar river on August 4th, 1995. The dashed plot shows a simulated fish track. Large uncertainties at the end of the track are due to very low signal to noise ratios (see figure 30).

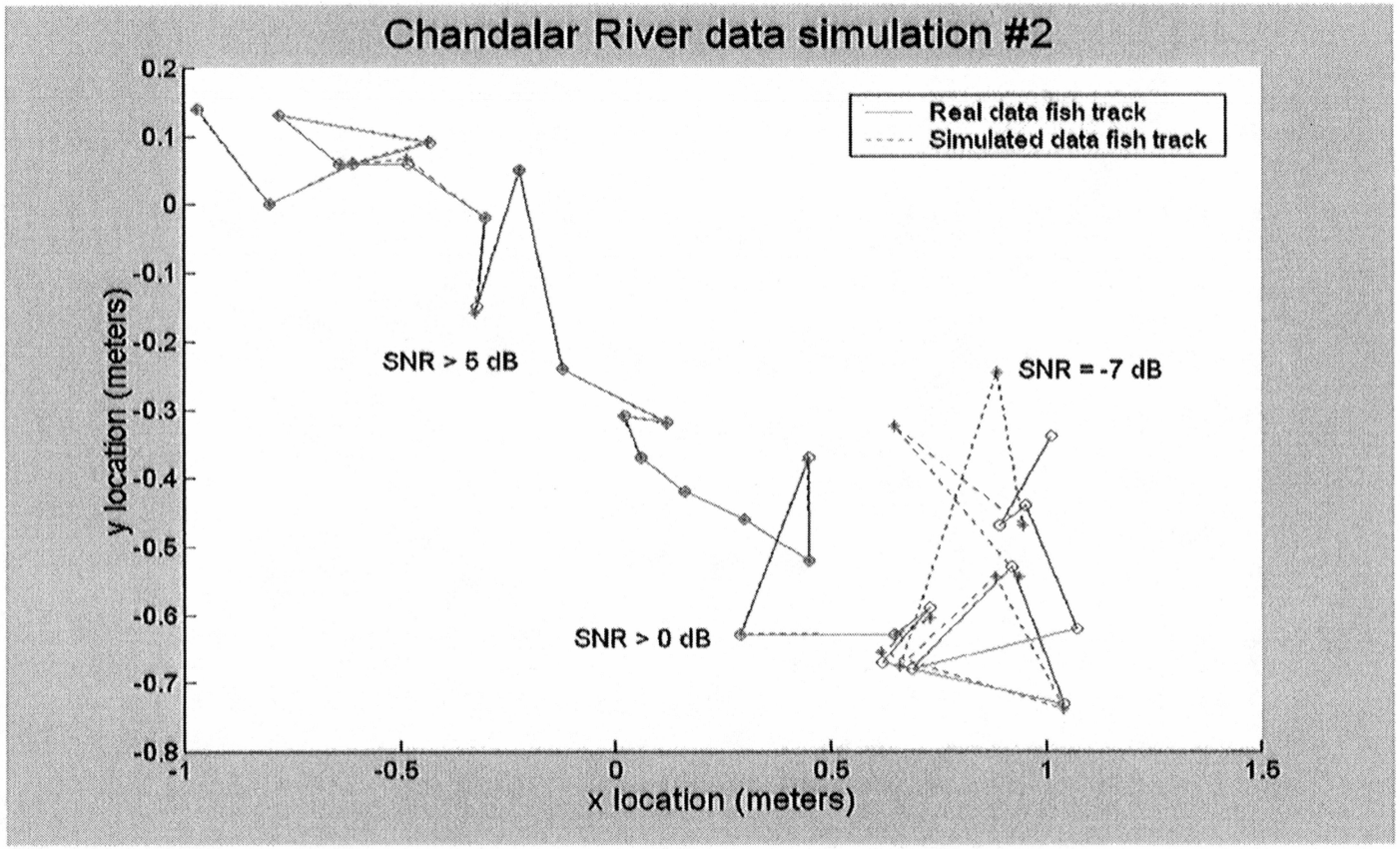

Figure 28. Chandalar River data simulation #2. This figure shows data collected from Chandalar river on August 4th, 1995. The dashed plot shows a simulated fish track. Large uncertainties at the end of the track are due to very low signal to noise ratios (see figure 30).

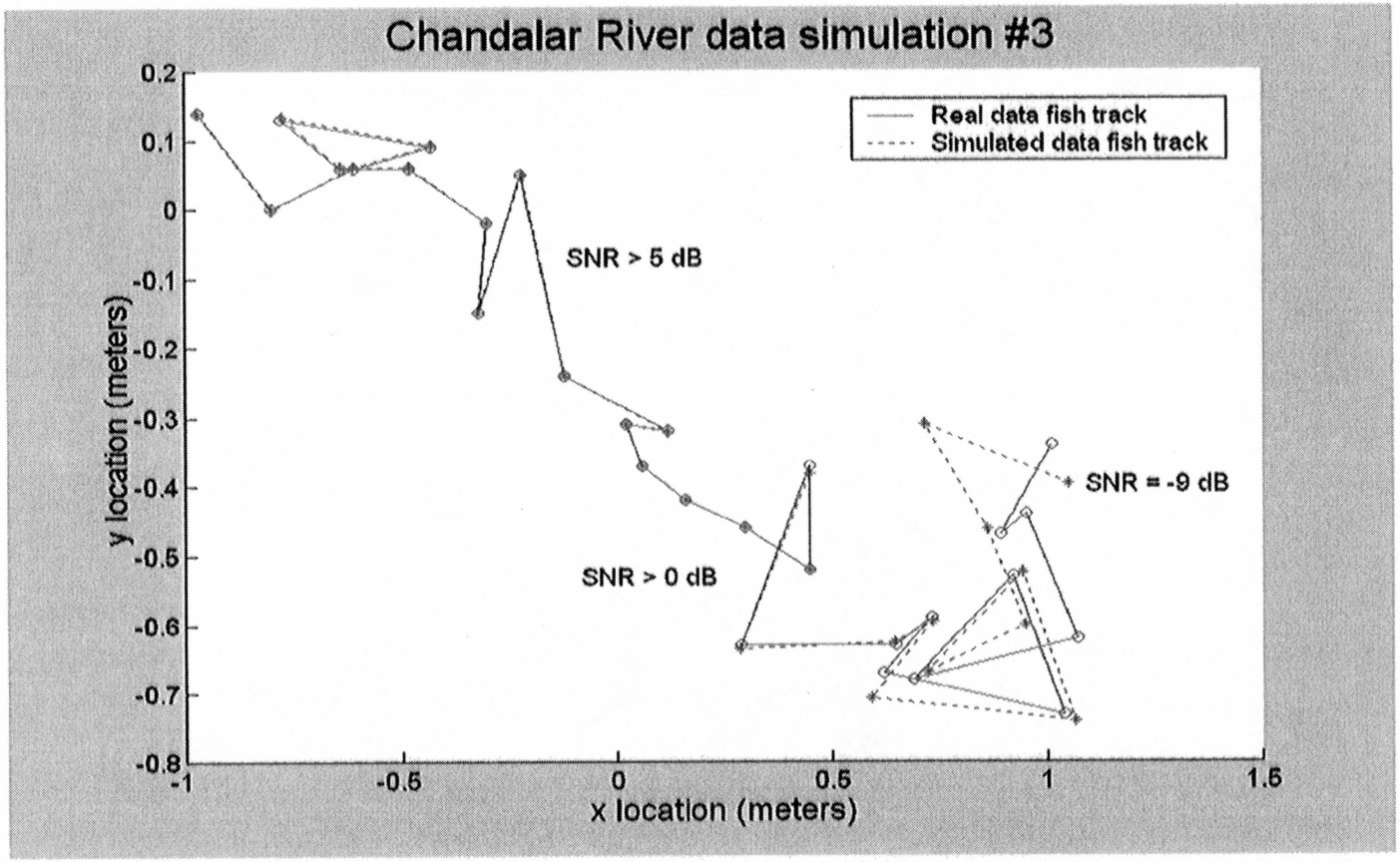

Figure 29. Chandalar River data simulation #3. This figure shows data collected from Chandalar river on August 4th, 1995. The dashed plot shows a simulated fish track. Large uncertainties at the end of the track are due to very low signal to noise ratios (see figure 30).

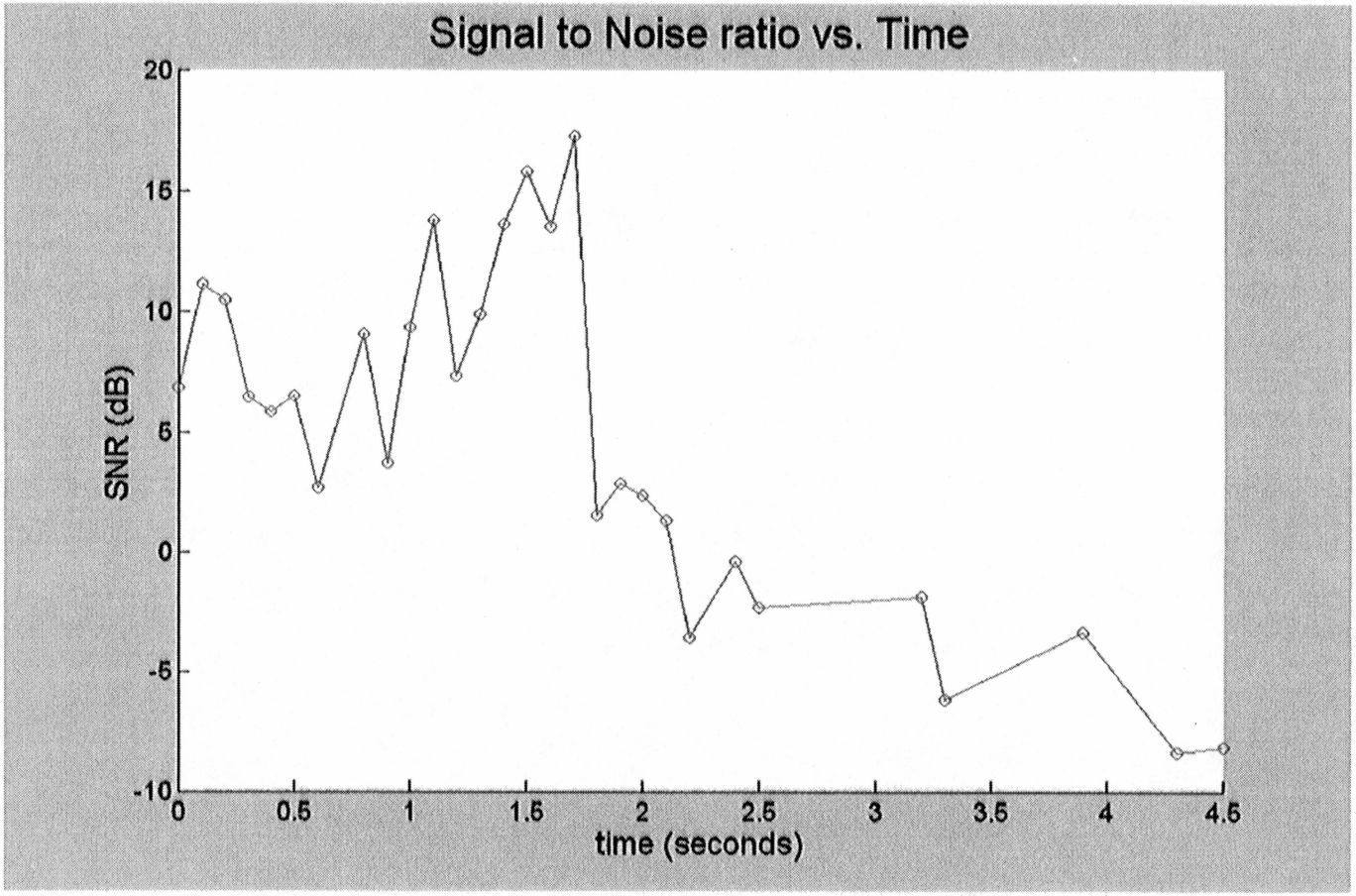

Figure 30. Signal to noise ratio vs. time for Chandalar River data. As the signal to noise ratio drops below 5 dB in the measured echoes, the uncertainty in fish location becomes significant with respect to the size of the fish and its estimated location.

4 Conclusions and Discussion

Modeling of the split beam sonar system provides insight into the system operation. The most significant result is the dependence of fish location estimates on signal to noise ratio. If the signal to noise ratio is lower than about 5 dB, then the fish location estimate becomes poor. The main sources of error in fish location are due to phase measurement error and range measurement error. Range measurement error can lead to phase wrap ambiguities. If the range estimate is poor, then the proper phase wrap will be difficult to determine and large errors can occur in the location estimate. If the sidelobes of the transducer beam are sufficiently low and the transducer is a rectangular array, then the phase wrap ambiguity can be removed by simply not including echoes which have a received level below some established threshold. If the sidelobes of the transducer are not lower than the maximum variation in the received target strength, then some fish will be excluded by the established threshold. The received target strength can vary by as much as 30 dB and is dependent on the orientation of the fish with respect to the sonar transducer.

The sampling frequency affects the quality of the location estimate. If the sampling frequency used to capture the noisy pulse is not greater than $5f_c$, noise can cause poor phase and range measurements which can lead to phase wrap ambiguities. If a large (greater than $5f_c$) sampling frequency is used more averaging will occur within the data and errors in the pulse due to noise will tend to cancel out. Filtering of the data does not appear to affect this sampling frequency requirement.

The duration of the transmitted pulse also affects the location uncertainty. Uncertainties due to selecting a pulse duration which is less than 100 waveform cycles can produce errors that are significant with respect to the scale of the fish track. Selecting

a pulse duration greater than 100 waveform cycles provides adequate averaging for reliable fish location estimate results.

The size of the individual fish being located affects the location estimate. A large fish will provide a greater target strength than a comparatively smaller fish. The target strength of the fish is directly related to the received signal to noise ratio, which is the most important parameter in fish location estimation. The size of the fish also affects the shape of the received pulse. A large fish will contribute more pulse spreading to the received pulse than a comparatively smaller fish. This difference in received pulse duration can cause errors in the calculation of the received pulse phase.

There are areas in this thesis where more research is required. The most important area is in the phase wrap determination algorithm. It has been shown that if the range estimate is incorrect, then the entire fish location estimate will be poor because of phase wrap ambiguities. More sophisticated filtering of the data and creative techniques for measuring the arrival time are suggested for improving the range measurement. The phase wrap problem can also be approached by looking at the returned echo level and excluding echoes with a level below some threshold. A combination of range estimating and echo level thresholding techniques may provide adequate results.

A better noise model is required to understand the uncertainties in the system completely. The model presented in this thesis models reverberation and background noise as Gaussian distributed random noise. Other noise sources such as flow noise and receiver noise are assumed to have levels much lower than reverberation and background noise. The Gaussian noise distribution presented here is a simple model for reverberation.

The rise/fall time of the pulse is assumed to be a constant value of 0.1 ms in this

thesis. This is not true for real fish echoes. Future work should include modeling the effect of both pulse rise/fall times due fish the fish flesh/swim bladder interface and pulse elongation due to fish size.

Different transducer types, including circular and elliptical transducers should be modeled. The simple rectangular transducer modeled in this thesis is only one of many transducer types used in practice. Transducer design methods such as shading should also be examined to model achievable sidelobe level reductions.

The behavior and movement of the fish should also be modeled. The fish tracks presented here are contrived examples to show the variation of location estimate with signal to noise ratio. The orientation of the fish in the beam in the two tracks presented in this thesis are constant and not necessarily representative of real fish behavior. The track simulated using the Chandalar River data set uses measured values of target strength and beam factor in the calculation of signal to noise ratio. The algorithms developed in this thesis provide means for calculating the target strength of a fish given any orientation and position. Using a fish behavior model to simulate tracks and provide orientation and location information, these tools can be used to simulate uncertainty in fish location using a split beam sonar.

Thus, problem of determining the uncertainty in fish location using a split beam sonar is not completely solved. This thesis provides a simulation model and some results related to simple examples. More work is required to fully quantify the uncertainty in a split beam sonar system in the presence of noise.

5 Appendix: Model Derivations

5.1 Transducer Beam Pattern

The transducer beam pattern used in this thesis is calculated by modeling the transducer as a two dimensional rectangular array.

An analytic expression can be written for a one dimensional linear array [Skolnik 1962]. The expression for a one dimensional linear array is:

$$b(\theta) = \frac{\sin(\frac{m\pi d_1}{\lambda}\sin\theta)}{m\sin(\frac{\pi d_1}{\lambda}\sin\theta)} \tag{40}$$

Where m is the number of array elements, d_1 is the separation between array elements, λ is the acoustic wavelength, and θ is the off-axis angle to the target.

This one dimensional linear array is extended to a two dimensional rectangular array for the thesis model. Since the two dimensional rectangular array is just a product of two one dimensional linear arrays [Skolnik 1962], we have:

$$b(\theta_1,\theta_2) = \frac{\sin(\frac{m\pi d_1}{\lambda}\sin\theta_1)}{m\sin(\frac{\pi d_1}{\lambda}\sin\theta_1)} \cdot \frac{\sin(\frac{n\pi d_2}{\lambda}\sin\theta_2)}{n\sin(\frac{\pi d_2}{\lambda}\sin\theta_2)} \tag{41}$$

Where m, n are the number of array elements in the θ_1 and θ_2 directions respectively, d_1, d_2 are the transducer separations and λ is the acoustic wavelength.

In the simulations performed in this thesis, θ_1 is in the X-Z plane and represents the left/right off axis angle. θ_2 is in the Y-Z plane and represents the up/down off axis angle. Figure 31 shows a three dimensional plot of the beam pattern used in the simulations. The parameters used to create this beam pattern are, $d_1 = 10$ cm, $d_2 = 10$ cm, m = 32, n = 32, and $\lambda = 1.25$ cm.

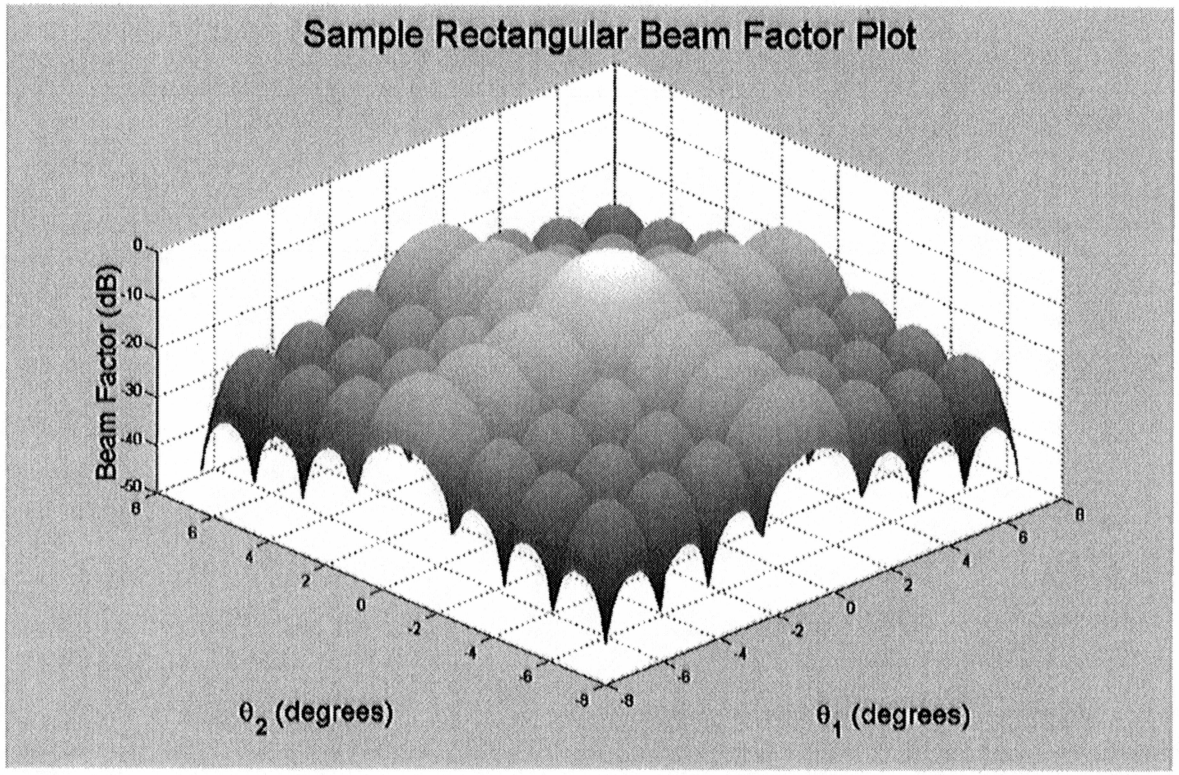

Figure 31. Two dimensional rectangular beam pattern used in simulations. A two-dimensional rectangular transudcer is simulated with 32 elements in the θ_1 direction and 32 elements in the θ_2 direction. The array elements are separated by 10 cm in both directions and the wavelength of transmission is 1.25 cm.

5.2 Low-pass and Band-pass Filters

The filters used to filter the simulated modulated and demodulated received pulses are developed in this section.

A band-pass FIR (finite impulse response) filter is used to reduce the noise in the received modulated pulse. The filter is designed by taking a pass-band that has parameters $f_{low} = 0.98f_c$ and $f_{hi} = 1.02f_c$. The filter order can be varying to achieve the desired roll-off around the filter's center frequency f_c. Trial and error experimentation shows that an order of about 40 provides adequate noise rejection and system speed. Figure 32 shows a plot of an ideal band-pass filter response along with the response for other finite order filters. The width of the band-pass filter must be finite (greater than zero) because the received pulse has finite rise/fall times which contribute spectral content at frequencies other than f_c. The low-pass filter used to filter the demodulated received pulse is designed in the same manner as the band-pass filter used to filter the modulated pulse. The low-pass filter cut-off frequency is set to $f_{low} = 0.02f_c$. The filters used to reduce the noise level in the data are simple and can certainly be improved with more research. These filters were chosen because of the simplicity of design and ease of implementation.

5.3 Coordinate System Transformations

The coordinate systems defined in this thesis are described in this section. Three different coordinate systems are used to describe the river, sonar and fish reference frames. The sonar and fish coordinate systems are referenced to the river system in all of the calculations.

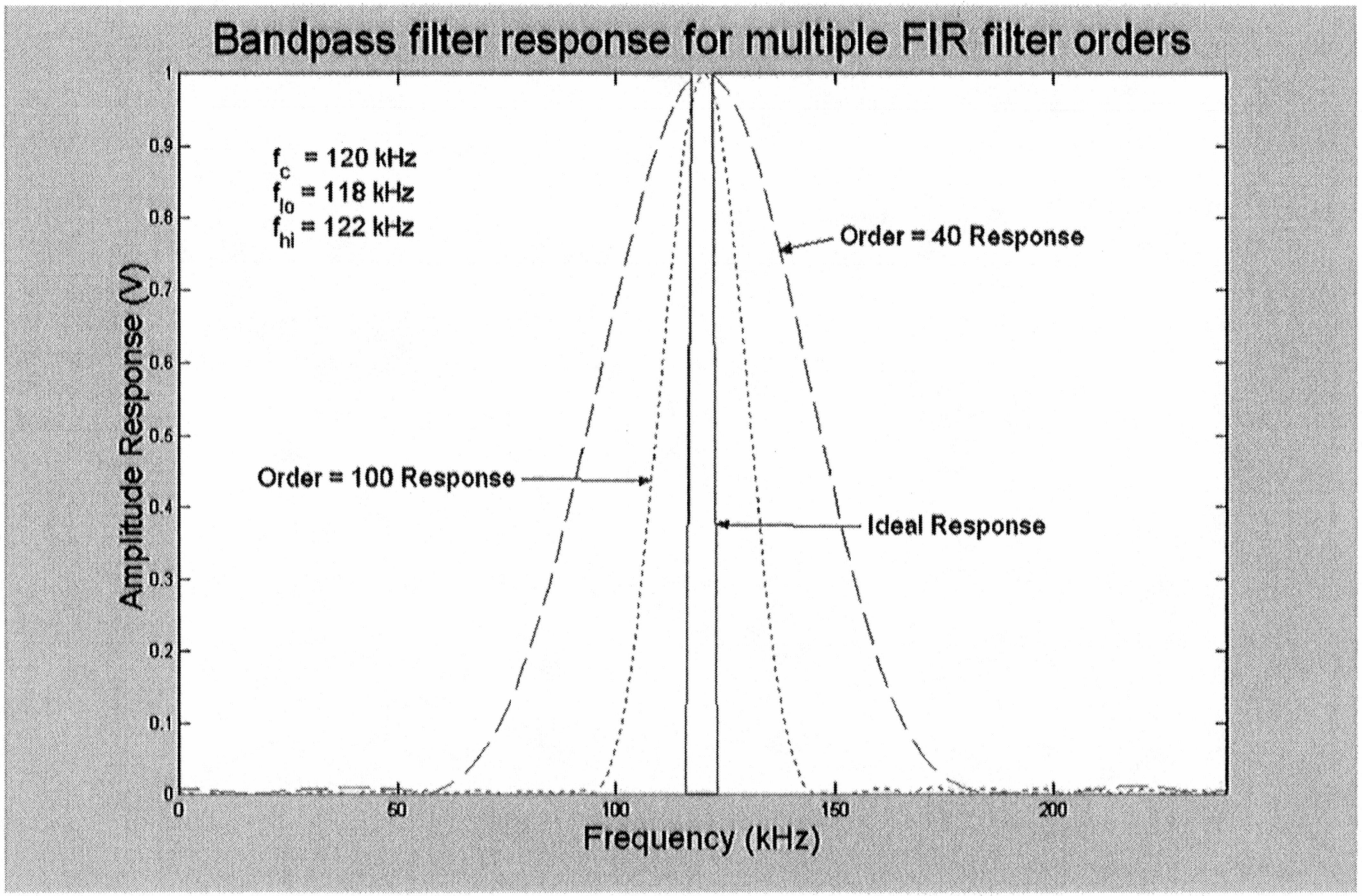

Figure 32. Band-pass filter response examples. An ideal band-pass filter response is shown along with two finite order FIR filter responses. The order of the filter used was selected by trial and error.

5.3.1 River System

The river coordinate system $[X_R\ Y_R\ Z_R]^T$ is defined with the z-axis perpendicular to the river bank and pointed away from the sonar location.The river y-axis is defined vertically upward and the x-axis is given by the right hand rule. In vector notation, the river system can be written as:

$$X_R = [1 \quad 0 \quad 0] \tag{42}$$

$$Y_R = [0 \quad 1 \quad 0] \tag{43}$$

$$Z_R = [0 \quad 0 \quad 1] \tag{44}$$

5.3.2 Sonar System

The sonar system is defined to allow the sonar to be tilted downward into the river, as is usually the case. Z_S is in the direction of the sonar beam axis. Y_S is in the Y_R - Z_R plane and is perpendicular to Z_S. X_S is given by the right hand rule. The angle θ_S is the of tilt in the Y_R - Z_R plane. Figure 10 shows the sonar system in terms of the Y_R - Z_R plane.

The sonar axes can be expressed in terms of the river axes as follows.

$$Z_S = Z_R \cos(\theta_S) - Y_R \sin(\theta_S) \tag{45}$$

$$Y_S = Z_R \sin(\theta_S) + Y_R \cos(\theta_S) \tag{46}$$

$$X_S = Y_S \times Z_S \tag{47}$$

5.3.3 Fish System

The fish coordinate system is defined with Z_F in the direction of the fish from tail to head. The Y_F axis is perpendicular to the Z_F axis and is in the direction of the dorsal fin. The X_F axis is given by the right hand rule. Figure 11 shows the fish coordinate system in terms of the river coordinate system.

The fish coordinate axes can be expressed in terms of the river axes by:

$$Z_F = X_S \sin(\theta_v)\cos(\phi_h) + Y_S \cos(\theta_v) + Z_S \sin(\theta_v)\sin(\phi_h) \tag{48}$$

$$Y_F = X_S \cos(\theta_v)\cos(\phi_h) + Y_S \sin(\theta_v) + Z_S \cos(\theta_v)\sin(\phi_h) \tag{49}$$

$$X_F = Y_F \times Z_F \tag{50}$$

Where X_S, Y_S and Z_S are the sonar system axes and θ_v, ϕ_h are the spherical angles defined in figure 11.

The fish can also be rolled about the Z_F axis by applying the following transformations:

$$X'_F = X_F \cos(\theta_{roll}) + Y_F \sin(\theta_{roll}) \tag{51}$$

$$Y'_F = Y_F \cos(\theta_{roll}) - Y_F \sin(\theta_{roll}) \tag{52}$$

Where θ_{roll} is the angle of roll about the Z_F axis.

5.4 Matched Filtering for Pulse Amplitude Estimation

A matched filter is used in one of the algorithms developed to estimate the pulse arrival time. The matched filtering algorithm estimates the peak returned voltage by convolving the received pulse with a modeled expected pulse.

Using the calculated peak received voltage, an arrival voltage is set as 90% of the peak voltage. The pulse delay is calculated as the time when the first occurrence of a voltage greater than 90% of the peak voltage is observed by the receiver.

A rectangular pulse with amplitude A and duration T_D is constructed to perform the matched filtering operation. Since the returned pulse will have a form very similar to the transmitted pulse, the peak correlation will occur when the pulses completely overlap. The filtering operation is performed in the frequency domain to increase speed. Figure 33 shows a block diagram of the matched filtering procedure.

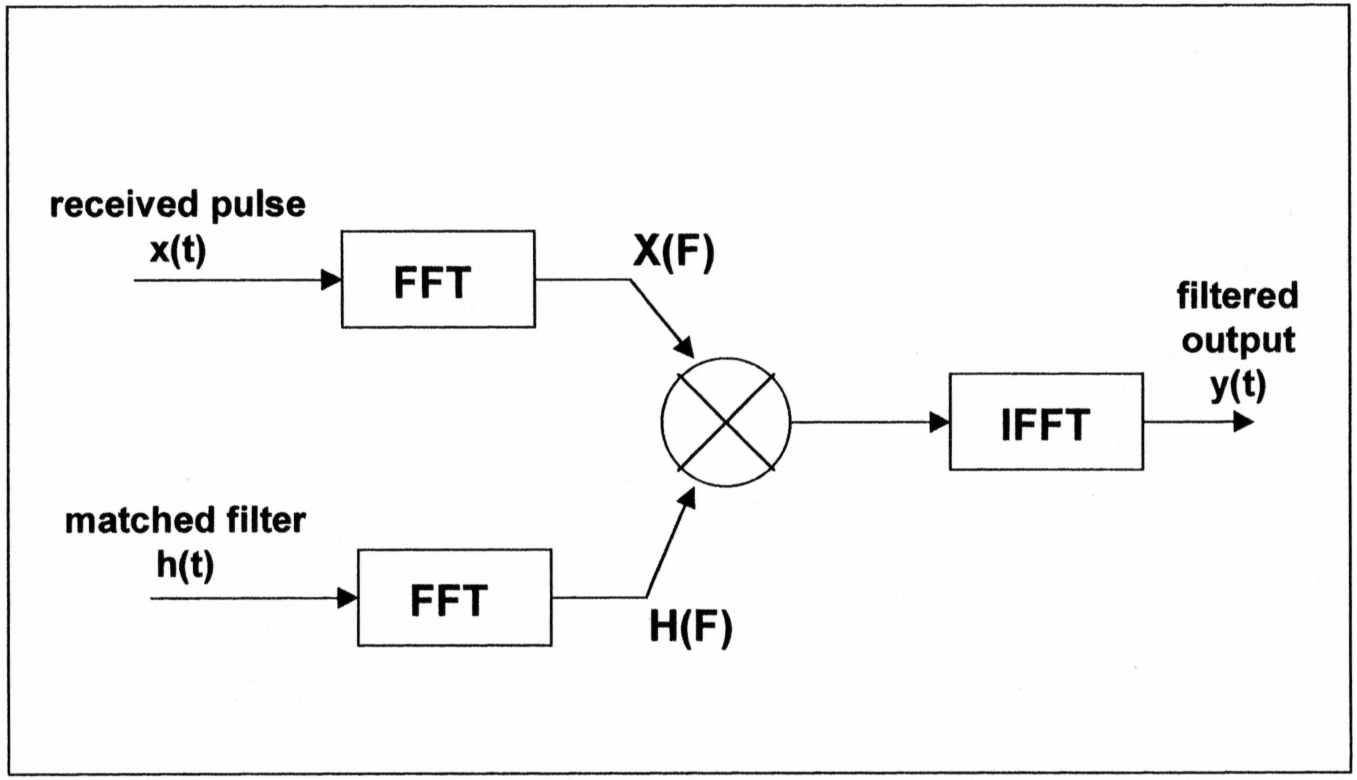

Figure 33. Matched filtering block diagram. The matched filtering operation consists of convolving the received pulse with a pulse created based on the parameters of the transmitted pulse. The peak correlation occurs when the two pulse overlap completely. The peak amplitude is calculated from the ouput y(t).

References

[Ayers 2001] Ayers, Mark L. 2001 A Guide to the Numerical Implementation of Split Beam Sonar, a report submitted for the partial fufillment of course EE 699. University of Alaska Fairbanks, March 2001

[Burdic 1991] Burdic, William S. 1991 Underwater Acoustic System Analysis, Prentice Hill Inc.

[Carlson 1986] Carlson, A. Bruce. 1986 Communications Systems: An Introduction to Signals and Noise in Electrical Communication, McGraw-Hill Inc.

[Daum and Osborne 1996] Daum, Dave W. and Osborne, Bruce M. 1996. Enumeration of Chandalar River Fall Chum Salmon using Split-Beam Sonar. Alaska Fisheries Progress Report Number 96-2.

[Ehrenberg 1981] Ehrenberg, John E. 1981. Analysis of split beam backscattering cross section estimation and single echo isolation techniques. Applied Physics Laboratory, University of Washington.

[Ehrenberg 1983] Ehrenberg John E. 1983. A Review of in situ target strength estimation techniquies. Applied Physics Laboratory, University of Washington, Seattle.

[Ehrenberg and Torkelson 1996] Ehrenberg, John E. and Torkelson, Thomas C. 1996. Applications of dual-beam and split-beam

target tracking in fisheries acoustics. ICES Journal of Marine Science, 53: 329-334.

[Ehrenberg 2000] Ehrenberg, John E. 2000. A signal processing description of acoustic echo sounding systems. Hydroacoustic Technology Inc.

[MacLennan et al., 1992] MacLennan, D. and Simmonds, John E. 1992 Fisheries Acoustics, Chapman Hall

[Nielson 1991] Nielson, Richard O. 1991 Sonar Signal Processing, Artech House Inc.

[Pham 1999] Pham, J. 1999 Application of digital spectral analysis and Monte Carlo simulation to the measurement of signal characteristics. UAF, M.S. Thesis

[Skolnik 1962] Skolnik, Merrill I. 1962 Introduction to Radar Systems, McGraw-Hill Book Company

[Sonwalker et al., 1999] Sonwalkar, Vikas S., Adams, Barbara L. and Kelley, John J. 1999 Target Strength of Fish at Arbitrary Angle of Incidence at High Frequencies. Submitted to Journal of Acoustic Society of America, August 1999.

[Traynor and Ehrenberg 1990] Traynor, Jimmie J. and Ehrenberg, John E. 1990. Fish ans standard-sphere target-strength measurements obtained with a dual-beam and split-beam

echo-sounding system. -Rapp. P.-v. Reun. Cons. int. Explor. Mer, 189: 325-335.

[Urick 1983] Urick, Robert J. 1983 Principles of Underwater Sound, McGraw-Hill